



SCHOOL of
GRADUATE STUDIES
EAST TENNESSEE STATE UNIVERSITY

East Tennessee State University
Digital Commons @ East
Tennessee State University

Electronic Theses and Dissertations

Student Works

8-2011

Quenching of the Fluorescence of Tris (2 2-Bipyridine) Ruthenium(II) $[\text{Ru}(\text{bipy})_3]^{2+}$ by a Dimeric Copper(II) Complex.

Kevin E. Cummins

East Tennessee State University

Follow this and additional works at: <https://dc.etsu.edu/etd>

 Part of the [Inorganic Chemistry Commons](#)

Recommended Citation

Cummins, Kevin E., "Quenching of the Fluorescence of Tris (2 2-Bipyridine) Ruthenium(II) $[\text{Ru}(\text{bipy})_3]^{2+}$ by a Dimeric Copper(II) Complex." (2011). *Electronic Theses and Dissertations*. Paper 1347. <https://dc.etsu.edu/etd/1347>

This Thesis - Open Access is brought to you for free and open access by the Student Works at Digital Commons @ East Tennessee State University. It has been accepted for inclusion in Electronic Theses and Dissertations by an authorized administrator of Digital Commons @ East Tennessee State University. For more information, please contact digilib@etsu.edu.

Quenching of the Fluorescence of Tris (2,2'-Bipyridine) Ruthenium(II),
[Ru(bipy)₃]²⁺, by a Dimeric Copper(II) Complex

A thesis
presented to
the faculty of the Department of Chemistry
East Tennessee State University

In partial fulfillment
of the requirements for the degree
Master of Science in Chemistry

by
Kevin E. Cummins
August 2011

Jeffrey G. Wardeska, Ph.D., Chair
Cassandra Eagle, Ph.D.
Ningfeng Zhao, Ph.D.

Keywords: Ruthenium, [Ru(bipy)₃]²⁺, Dimeric Copper(II), Fluorescence, Quenching

ABSTRACT

Quenching of the Fluorescence of Tris (2,2'-Bipyridine) Ruthenium(II),

$[\text{Ru}(\text{bipy})_3]^{2+}$, by a Dimeric Copper(II) Complex

by

Kevin E. Cummins

The quenching of the $[\text{Ru}(\text{bipy})_3]^{2+}$ by Cu_2L^{2+} was studied and the data were plotted with the Stern-Volmer equation. The plot showed a break and was divided into 2 regions, <0.5 and >0.5 $\text{Cu}_2\text{L}^{2+} : [\text{Ru}(\text{bipy})_3]^{2+}$ molar ratio. Quenching above the 0.5 $\text{Cu}_2\text{L}^{2+} : [\text{Ru}(\text{bipy})_3]^{2+}$ molar ratio was slower ($330 \times 10^{-6} \text{ M}^{-1}\text{s}^{-1}$) than the quenching rate reaction below 0.5 ratio ($387 \times 10^{-6} \text{ M}^{-1}\text{s}^{-1}$).

With Cu_2L^{2+} being a dimeric complex the break and differences in the quenching reaction rates can be explained in terms of the stoichiometry. When the $\text{Cu}_2\text{L}^{2+} : [\text{Ru}(\text{bipy})_3]^{2+}$ ratio is < 0.5 , then each $[\text{Ru}(\text{bipy})_3]^{2+}$ can interact with 1 Cu_2L^{2+} dimer. At 0.5 then there is exactly a 1:1 ratio $\text{Ru}^{\text{II}} : \text{Cu}^{\text{II}}$. Above the 0.5 ratio the $[\text{Ru}(\text{bipy})_3]^{2+}$ can interact with maybe only one of the Cu_2L^{2+} 's in the dimer, or with a $[\text{Ru}(\text{bipy})_3]^{2+} : \text{Cu}_2\text{L}^{2+}$ unit, so the quenching is less efficient.

ACKNOWLEDGEMENTS

I'd like to thank my research advisor Dr. Jeff Wardeska for all his guidance and knowledge he has given me during my time at ETSU. I would also like to thank the Chemistry department in general for providing a great learning environment.

Thanks also to Dr. Cassandra Eagle and Dr. Peter Zhao for their willingness to serve on my graduate committee. Thanks to Dr. Jiang for use of his lab and the Horiba Jobin Yvon UV-Vis spectrometer.

Thanks to the management at Unimin Corporation, especially Dr. Chris Capobianco, for his supportive and encouraging attitude that helped me to attain my degree while working.

Most of all, I would like to thank my lovely wife Tami Cummins for all the understanding, patience, love, and support that she has given me during my studies.

CONTENTS

	Page
ABSTRACT	2
ACKNOWLEDGEMENTS	3
LIST OF TABLES	6
LIST OF FIGURES	7
LIST OF STRUCTURES	9
Chapter	
1. INTRODUCTION	10
Fluorescence of Tris (2,2'-Bipyridine) Ruthenium(II) Complexes	10
Electron Transition	11
Quenching	15
Project Goal	18
2. EXPERIMENTAL SECTION	19
Physical Measurements	19
Materials	21
Preparations	21

Absorbance Measurements	25
Emission Analyses	26
3. RESULTS	30
4. DISCUSSION AND CONCLUSION	44
5. RECOMMENDATION	47
REFERENCES	48
APPENDICES	50
Appendix A: UV-Vis absorbance test results	50
Appendix B: Measured fluorescence data for $\text{Cu}_2\text{L}^{2+}:\text{[Ru(bipy)}_3\text{]}^{2+}$ ratios in 0.1M KNO_3 , 25°C (1st Repeat)	51
Appendix C: Measured fluorescence data for $\text{Cu}_2\text{L}^{2+}:\text{[Ru(bipy)}_3\text{]}^{2+}$ ratios in 0.1M KNO_3 , 25°C (2nd Repeat)	52
6. VITA	53

LIST OF TABLES

Table	Page
1. Cu_2L^{2+} - $[\text{Ru}(\text{bipy})_3]^{2+}$ ratios in 0.1 M KNO_3	28
2. Cu_2L^{2+} - $[\text{Ru}(\text{bipy})_3]^{2+}$ ratios in 0.1 M KNO_3	29
3. UV-Vis absorbance test results	50
4. Measured fluorescence data for $\text{Cu}_2\text{L}^{2+}:[\text{Ru}(\text{bipy})_3]^{2+}$ ratios in 0.1 M KNO_3 , 25°C	36
5. Calculation of quenching rate constants (k_q) of Cu_2L^{2+} on $[\text{Ru}(\text{bipy})_3]^{2+}$ (2.23 mM)	39
6. Calculation of quenching rate constants (k_q) of Cu_2L^{2+} on $[\text{Ru}(\text{bipy})_3]^{2+}$. Horiba UV-Vis results	43
7. Measured fluorescence data for $\text{Cu}_2\text{L}^{2+}:[\text{Ru}(\text{bipy})_3]^{2+}$ ratios in 0.1M KNO_3 , 25°C (1st Repeat)	51
8. Measured fluorescence data for $\text{Cu}_2\text{L}^{2+}:[\text{Ru}(\text{bipy})_3]^{2+}$ ratios in 0.1M KNO_3 , 25°C (2nd Repeat)	52

LIST OF FIGURES

Figure	Page
1. Possible electron transitions during absorption for d-block complexes	12
2. The absorption and emission data of $[\text{Ru}(\text{bipy})_3]^{2+}$	13
3. Jablonski diagram for ruthenium polypyridyl complexes	15
4. Absorption spectrum of $[\text{Ru}(\text{bipy})_3](\text{BF}_4)_2 \cdot 4\text{H}_2\text{O}$	31
5. Absorption spectrum of $[\text{C}_{22}\text{H}_{20}\text{Br}_2\text{Cu}_2\text{N}_4\text{O}_2]^{2+}(\text{Cl}_2)$	32
6. Emission intensity semi-quantitative heating study results	34
7. Comparison of Ar purged samples with non-purged samples	35
8. Emission intensity decrease as a result of Cu_2L^{2+} quenching on $[\text{Ru}(\text{bipy})_3]^{2+}$, 25°C. $[\text{Ru}(\text{bipy})_3]^{2+} = 2.23 \text{ mM}$	37
9. Stern-Volmer plot of the relative fluorescence intensities	38
10. Emission Intensity decrease as a result of Cu_2L^{2+} quenching on $[\text{Ru}(\text{bipy})_3]^{2+}$, 25°C. $[\text{Ru}(\text{bipy})_3]^{2+} = 2.23 \text{ mM}$	40
11. Stern-Volmer plot of the relative fluorescence intensities at 25°C analyzed with the Horiba Jobin Yvon UV-Vis spectrometer	40

12. Emission Intensity decrease as a result of Cu_2L^{2+} quenching on $[\text{Ru}(\text{bipy})_3]^{2+}$, 30°C. $[\text{Ru}(\text{bipy})_3]^{2+} = 2.23 \text{ mM}$	41
13. Stern-Volmer plot of the relative fluorescence intensities at 30°C analyzed with the Horiba Jobin Yvon UV-Vis spectrometer	41
14. Emission Intensity decrease as a result of Cu_2L^{2+} quenching on $[\text{Ru}(\text{bipy})_3]^{2+}$, 40°C. $[\text{Ru}(\text{bipy})_3]^{2+} = 2.23 \text{ mM}$	42
15. Stern-Volmer plot of the relative fluorescence intensities at 40°C analyzed with the Horiba Jobin Yvon UV-Vis spectrometer	42

LIST OF STRUCTURES

Structure	Page
1. $[\text{Ru}(\text{bipy})_3](\text{BF}_4)_2$	30
2. $[\text{C}_{22}\text{H}_{20}\text{Br}_2\text{Cu}_2\text{N}_4\text{O}_2^{2+}](\text{Cl}_2)$	31

CHAPTER 1

INTRODUCTION

In the ultimate plan of coupling tris (2,2'-bipyridine) ruthenium(II), $[\text{Ru}(\text{bipy})_3]^{2+}$, to a dibromo-functionalized dimeric copper(II) chloride complex of 7,11;19,23-dimetheno-9,21-dibromo[1,5,13,17]-tetra-azacycloicosa-5,7,9,12,17,19,21,24-octaene-25,26-diol, $(\text{C}_{22}\text{H}_{20}\text{Br}_2\text{Cu}_2\text{N}_4\text{O}_2)\text{Cl}_2$ or Cu_2L^{2+} , the interaction of the two separate complexes were investigated.

Fluorescence of Tris (2,2'-Bipyridine) Ruthenium(II) Complexes

Luminescence can be defined as light that usually occurs at low temperature and is a form of cold body radiation. Luminescence can be produced from chemical reactions, electrical energy, subatomic motions, or stress on a crystal. ⁽¹⁾ Fluorescence is a form of luminescence that is defined as the emission of light by a substance that has absorbed light or other electromagnetic radiation of a different wavelength. ⁽²⁾

In 1959, Paris and Brandt reported the first observation of fluorescence from *tris* (2,2'-bipyridine) ruthenium(II), $[\text{Ru}(\text{bipy})_3]^{2+}$. In order for fluorescence (i.e. electron transfer) to occur a photon of light must excite the $[\text{Ru}(\text{bipy})_3]^{2+}$ to an excited state, $^*[\text{Ru}(\text{bipy})_3]^{2+}$. In the excited state the $^*[\text{Ru}(\text{bipy})_3]^{2+}$ possesses enough energy to undergo fluorescence. ⁽³⁾ The fluorescence was assigned to the decay of an excited state of the molecule produced by MLCT (Metal to Ligand Charge Transfer) absorption, $(t_{2g})^6 \rightarrow \pi^*$. ^(4, 5)

Electron Transition

Inorganic molecules, or more specifically d-block complexes, add an extra layer of molecular orbitals between the ligand π orbital and an excited state ligand π^* orbital. Illustrated in Figure 1, electron transitions are called ligand-field or ligand-ligand transition, in the excited state the electron is located on the ligand. Because of the presence of the metal's molecular orbitals, three other transitions are available – a d-d transition, where an electron is excited from a metal d orbital to an unoccupied metal d orbital (this is usually referred to as a metal centered transition) as well as transitions between the metal and the ligand. These can involve either an electron excited from the ligand to the metal, called Ligand to Metal Charge Transfer (LMCT), or from the metal to the ligand (MLCT). Because of the energy differences between the various types of transitions, ligand field transitions are usually in the visible near-UV region, and charge transfer transitions are much more intense with the resulting emission often being highly colored.

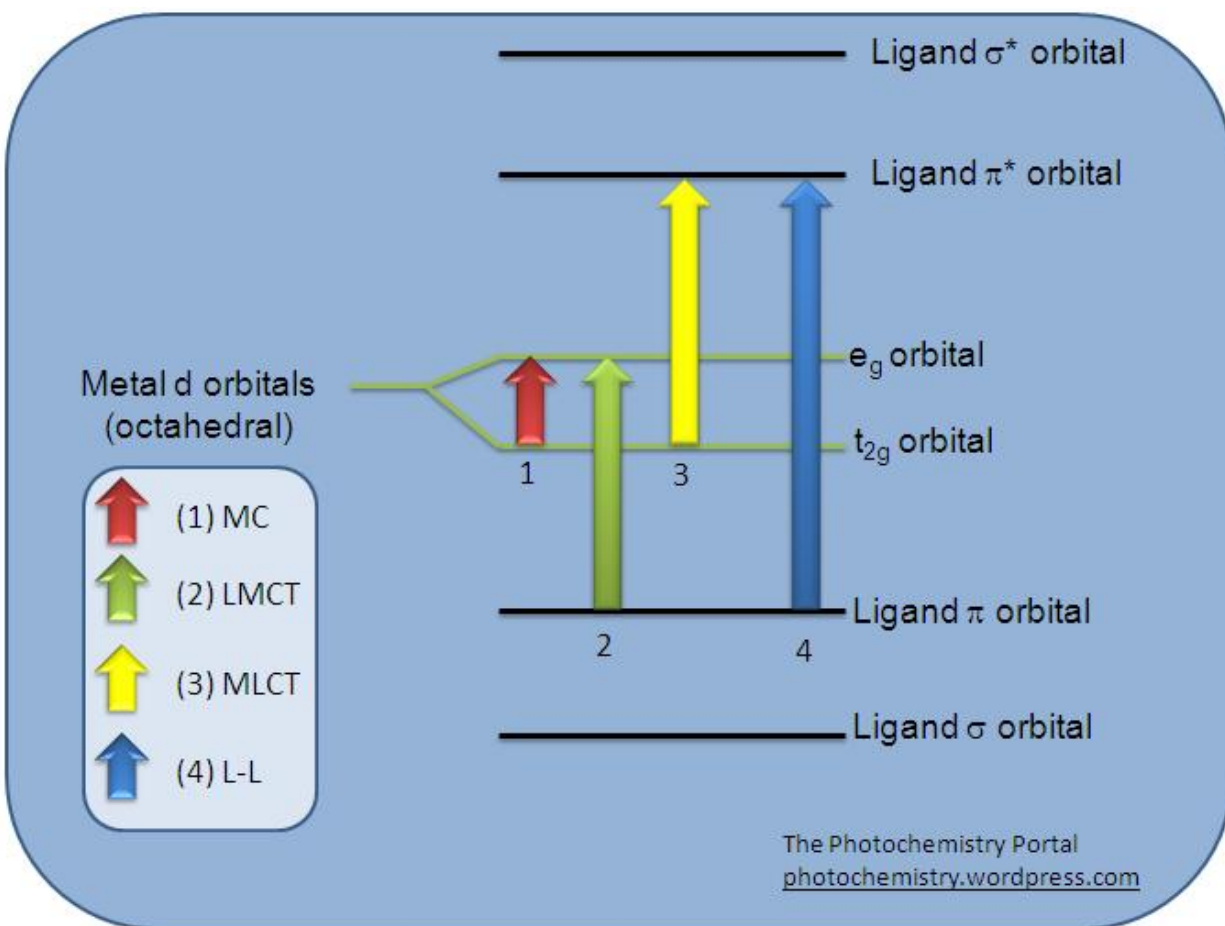


Figure 1. Possible electron transitions during absorption for d-block complexes.⁽⁶⁾

Ruthenium in oxidation state II is a d^6 element and typically forms octahedral complexes in which the electrons are in the low-spin t_{2g}^6 configuration. Incident light at about 450 nm promotes one of these electrons to a ligand anti-bonding orbital, a metal to ligand charge transfer as Figure 2 shows.

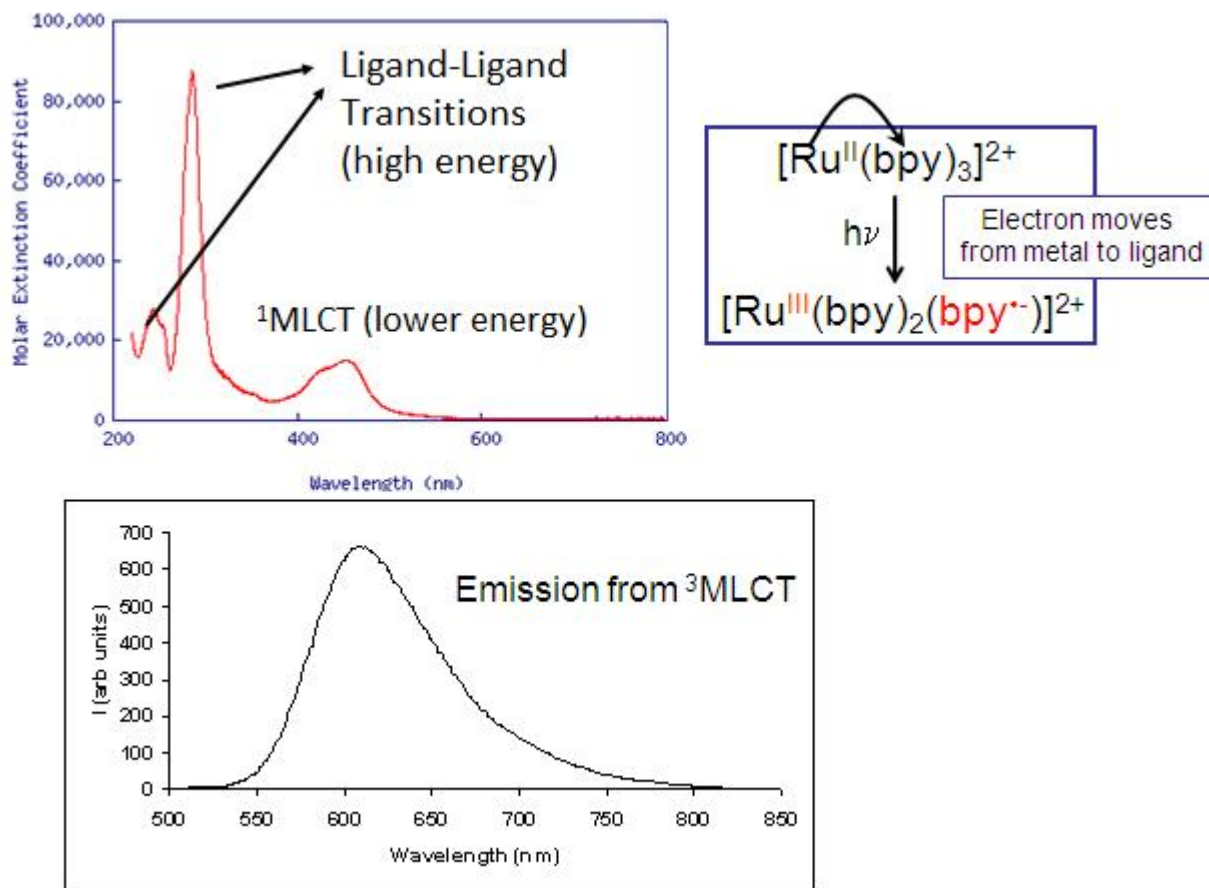


Figure 2. The absorption and emission data of $[\text{Ru}(\text{bipy})_3]^{2+}$.⁽⁶⁾

Ruthenium absorbs energy at 450 nm and emits strongly at ~620 nm in water.

This emission is caused by radiative process from the $^3\text{MLCT}$ state to the ground state.

Emission lifetimes are approximately 600 ns in deaerated water.⁽⁶⁾

As seen in Figure 3, the excited state is labeled $^1\text{MLCT}$. In the excited state, $^*[\text{Ru}(\text{bipy})_3]^{2+}$ has enough energy to undergo an electron transfer or to fluoresce.⁽³⁾ Energy transfer to $^3\text{MLCT}$ is efficient (heavy atom effect) and so ruthenium complex's photochemistry generally happens from here. Essentially, heavy atom effect is when

atoms with high atomic number cause spin selection rules to be less rigidly obeyed due to spin-orbit coupling.

The excitation of electrons can occur with or without a change in spin of the electron. A singlet state is produced if the spin is not changed in a molecule containing no unpaired electrons so both the excited state and ground state have a multiplicity of one. The multiplicity is given by two times the sum of the individual spins, m_s , plus one: $2S + 1 = 2\sum m_s + 1$. A triplet state can result if the spin of the electron is changed in the transition so the excited state contains two unpaired electrons with identical magnetic spin quantum numbers therefore having a multiplicity of three. ⁽⁷⁾

For transition metal ion complexes there can be various kinds of electron-electron interactions in the excited state that are more complicated than the assumption that the transition involves a simple transfer of an electron from the ground state level to an empty excited state level. The excited state can have different electron-electron repulsions than those in the previously mentioned simple excitation transition. In addition to affecting the energy, these various kinds of excited state electron-electron interactions produce many more transitions than those predicted by the simple electron promotion system. These extra transitions would result because the levels that would otherwise be degenerate are split by electronic interactions. ⁽⁸⁾ Rusak et al. ⁽⁹⁾ point out the luminescence of $[\text{Ru}(\text{bipy})_3]^{2+}$ is produced from the ligand-to-metal charge transfer in which the emitting state has some degree of triplet character.

However, due to the high atomic number of Ru, these emitting states can be described as spin-orbit states rather than pure triplets or singlets.

Emission is caused by radiative process from the $^3\text{MLCT}$ state to the ground state. With the introduction of a quencher such as the Cu_2L^{2+} an electron transfers from the $^3\text{MLCT}$ to the ^3MC .

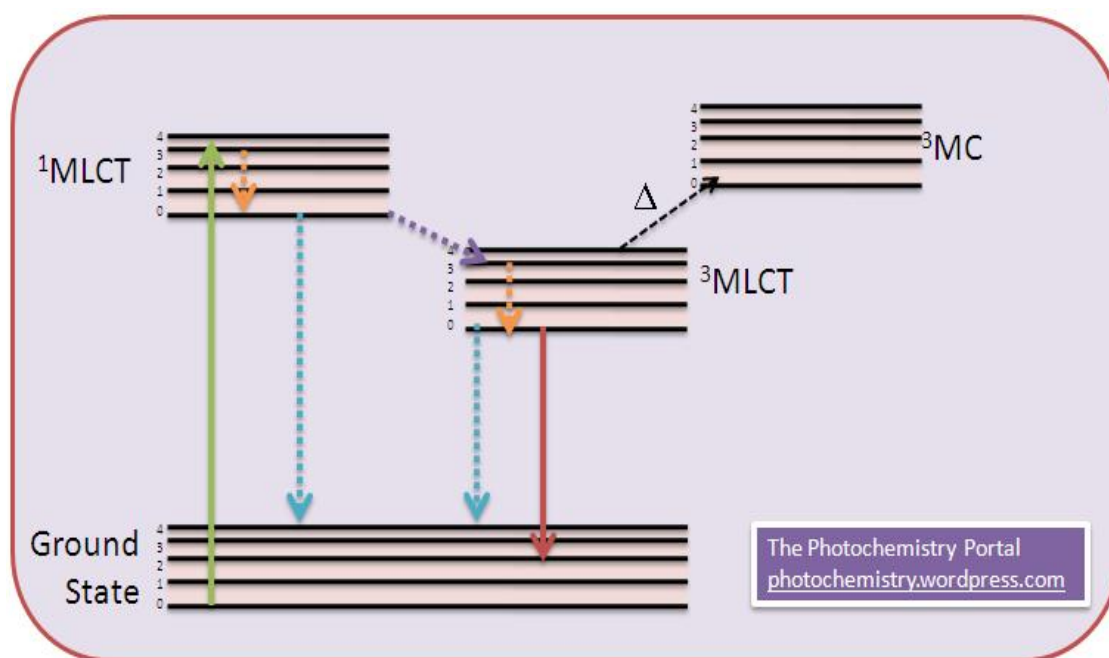


Figure 3. Jablonski diagram for ruthenium polypyridyl complexes. Solid lines and dashed lines are radiative and non-radiative processes respectively.⁽⁶⁾

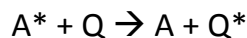
Quenching

Many model systems have been investigated to determine the rate constants and quenching mechanics on $[\text{Ru}(\text{bipy})_3]^{2+}$.^(3,9,10) Excited states can be deactivated in several ways. They can emit energy by giving off light energy, deactivate which results in a “vibrationally hot” ground state (*i.e.* energy loss as heat), or be quenched by another molecule.

Quenching refers to any process that decreases the fluorescence intensity of a given substance. The fluorescence is reduced through a radiationless process. ⁽³⁾

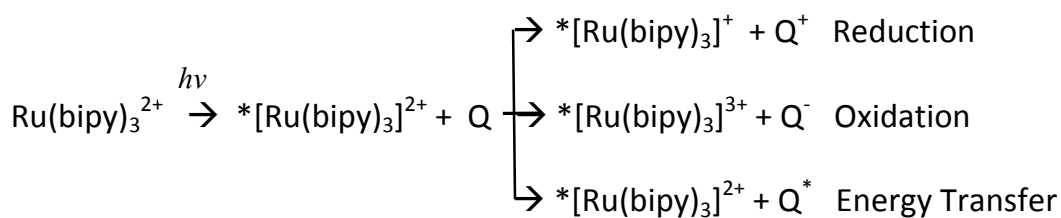


or



A = Chemical Species; Q = Quencher; * = Excited State

The quenching of $^*[\text{Ru}(\text{bipy})_3]^{2+}$ emission can be summarized by the following equations⁽¹¹⁾.



The kinetics of deactivation of the excited state follows the Stern-Volmer relationship. The Stern-Volmer equation is generated by quantifying the quantum yield of emission as being the rate constant of emission divided by the sum of all rate constants deactivating the excited state. The Stern-Volmer equation can then be simplified by dividing the emission quantum yield in the absence of quencher by that in the presence of quencher.

In absence of quencher

$$\Phi_f^0 = \frac{k_f}{k_f + k_d} = \frac{k_f}{\frac{1}{\tau_0}} = k_f \tau_0$$

In presence of quencher

$$\Phi_f = \frac{k_f}{k_f + k_d + k_q[Q]} = \frac{k_f}{\frac{1}{\tau_0} + k_q[Q]}$$

Dividing these equations

$$\frac{\Phi_f^0}{\Phi_f} = \frac{\frac{k_f}{\frac{1}{\tau_0}}}{\frac{k_f}{\frac{1}{\tau_0} + k_q[Q]}} = 1 + k_q \tau_0 [Q]$$

The Stern-Volmer equation then simplifies to equation 1:

$$\frac{\Phi_f^0}{\Phi_f} = \frac{\tau_0}{\tau} = \frac{I_0}{I} = 1 + k_q \tau_0 \cdot [Q] \quad [1]$$

I_0 = Intensity of $^*[\text{Ru}(\text{bipy})_3]^{2+}$ without a quencher

I = Intensity with a quencher

k_q = Quencher rate co-efficient

τ_0 = Fluorescence lifetime of $^*[\text{Ru}(\text{bipy})_3]^{2+}$ without a quencher

Q = Concentration of quencher

Schenk and Sherer investigated the effects of fluorescence quenching of the excited state $^*[\text{Ru}(\text{bipy})_3]^{2+}$ by copper(II) through electron transfer.⁽³⁾ The fluorescence spectra of the excited state $^*[\text{Ru}(\text{bipy})_3]^{2+}$ showed a maximum emission at 598 nm. The product $k_q \cdot \tau_0$ is often referred to as K_{sv} and for the reaction between Cu^{2+} and

*[Ru(bipy)₃]²⁺ was found to be 121 M⁻¹ and the k_q for the electron transfer rate constant for Cu²⁺ was found to be 212 M⁻¹s⁻¹.

In this experiment we studied the effects of using a dimeric Cu complex, Cu₂L²⁺, to quench the fluorescence of *tris*-(2,2'-bipyridine)ruthenium(II), [Ru(bipy)₃]²⁺. For [Ru(bipy)₃]²⁺ to fluoresce it must be in its excited state, *[Ru(bipy)₃]²⁺, which is accomplished by light photon excitation. Being in the excited state *[Ru(bipy)₃]²⁺ has enough energy to fluoresce (i.e. undergo electron transfer). Schenk et al. stated when *[Ru(bipy)₃]²⁺ is quenched with Cu²⁺, *[Ru(bipy)₃]²⁺ will most likely be oxidized.⁽³⁾ With our dimeric Cu complex, Cu₂L²⁺, we believe the quenching will most likely be by oxidation as well.

Project Goal

This study investigates the quenching efficiency of a dimeric copper (i.e. Cu₂L²⁺), complex on [Ru(bipy)₃]²⁺. The Cu₂L²⁺ quenching rate constant is determined through the use of the Stern-Volmer equation. Particular focus is also given to the confirmation of a break, using the Stern-Volmer plot, in the emission intensity that occurs at the 0.5 Cu₂L²⁺: [Ru(bipy)₃]²⁺ molar ratio.

CHAPTER 2

EXPERIMENTAL SECTION

Experiments were conducted to obtain UV-Vis absorbance spectra for both the $[\text{Ru}(\text{bipy})_3](\text{BF}_4)_2$ and the Cu_2L^{2+} complex. In an attempt to complex the $[\text{Ru}(\text{bipy})_3]^{2+}$ and Cu_2L^{2+} together as well as to study if pH might induce bridging of the compounds together experiments were conducted involving reacting the compounds in media of varying pH for analysis. Other experiments investigated the temperature effects on emission intensity for a series of $[\text{Ru}(\text{bipy})_3]^{2+}$ - Cu_2L^{2+} ratio mixtures and the effect of oxygen quenching of the $[\text{Ru}(\text{bipy})_3](\text{BF}_4)_2$. Determination of effects of ionic strength on the emission spectrum was also looked at. Using the Stern-Volmer relation the quenching constant rates were determined by plotting the $[\text{Ru}(\text{bipy})_3]^{2+}$: Cu_2L^{2+} molar ratios vs. emission intensity.

Physical Measurements

UV-Visible absorption spectra were recorded on a Shimadzu UV-2401PC UV-Vis spectrometer. The instrument was run in Spectrum mode with a wavelength range setting of 700 to 400nm.

Emission intensity measurements were performed using an Ocean Optics USB4000 UV-Vis spectrometer equipped with a LS-450 blue LED pulsed light source. The Ocean Optics spectrometer sampling system functions as follows.^(10,12)

The light from the light source transmits through an optical fiber to the sample where it interacts with the sample. Another optical fiber collects and transmits the result of the interaction to the spectrometer. The spectrometer measures the amount of light and transforms the data collected by the spectrometer into digital information. The spectrometer passes the sample information to SpectraSuite software. SpectraSuite compares the sample to the reference measurement and displays processed spectral information.

The analysis settings in the spectrometer software SpectraSuite were set at the following parameters: Scope Mode, Intensity time = 100 ms, 20 scans, boxcar = 100 while the emission at 617nm was evaluated. The parameters are defined as follows. ⁽¹²⁾

Integration time - Specifies the integration time of the spectrometer, which is analogous to the shutter speed of a camera. The higher the integration time, the longer the detector monitors the incoming photons. If the Scope mode intensity is too low, increase this value. If the intensity is too high, decrease this value.

Scans to average - Specifies the number of discrete spectral acquisitions that the device driver accumulates before SpectraSuite receives a spectrum. The higher the value, the better the signal-to-noise ratio (S:N). The S:N will improve by the square root of the number of scans averaged.

Boxcar - Sets the boxcar smoothing width, a technique that averages across spectral data. This technique averages a group of adjacent detector elements. A value of 5, for

example, averages each data point with 5 points to its left and 5 points to its right. The greater this value, the smoother the data and the higher the signal-to-noise ratio. If the value entered is too high, a loss in spectral resolution will result. The S:N will improve by the square root of the number of pixels averaged.

To correct for instrument response variables on the Ocean Optics spectrometer references and dark measurements were performed and stored before each daily analysis runs.

Emission intensity measurements at different temperatures were obtained on a Horiba Jobin Yvon UV-Vis spectrometer. The UV-Vis parameters were set with an incident light wavelength of 472 nm with an Integration time of 0.3, and a Slit width of 2.

Materials

All commercially available materials, Baker & Anderson (B & A) 30% hypophosphorous acid, Fisher Scientific S-318 NaOH pellets, Alfa Aesar ruthenium (III) chloride and 2,2'-bipyridine, were used without any further purification.

Preparations

Synthesis and characterization of tris (2,2'-bipyridyl ruthenium (II) tetrafluoroborate trihydrate (Structure I)

This compound was prepared by a modification of a procedure found in the literature.⁽¹⁴⁾ Hypophosphorous acid, H₃PO₂, (10 cm³) was pipetted with a Corex 7100-A

10 cm³ pipette into a 25 cm³ beaker with dionized water (6 cm³) added with a 10 cm³ Kinax pipette. A stirbar was placed in a solution and was stirred using a magnetic stirrer hotplate. The pH was determined using Hydrion Papers pH indicator (Micro Essential Laboratories) as a pH of <2. Sodium hydroxide, NaOH, pellets (2.3797 g, 0.0596 mols) were added until the pH of ~7 was indicated using Hydrion Papers pH indicator to form NaH₂PO₂.

Ruthenium(III) chloride, RuCl₃ · 3 H₂O, (0.1665 g, 6.369 x 10⁻⁴ mols) was dried at 110°C for 1 hour. The RuCl₃ · 3 H₂O was dissolved in 16 cm³ of dionized H₂O in a 30 cm³ beaker with a stirbar, then 2,2'-Bipyridine (0.3761 g, 2.408 x 10⁻³ mols) was added. Sodium hypophosphite solution, NaH₂PO₂, (0.88 cm³) made above was added to this solution using a Corex # 7064-A 1mL pipette. The solution was stirred at 700 rpm on a Fisher Scientific Isotemp hotplate with a stirrer. This solution was then refluxed for 30 minutes.

After refluxing, sodium tetrafluoroborate, NaBF₄, (0.6661g, 6.067 x 10⁻³ mols) dissolved in 3 cm³ of dionized water was added. This solution was cooled to room temperature then placed in an ice bath for further cooling and crystal formation. Crystals were washed with cold 95% ethanol.

For determination of percent water content 0.1000g of the crystals were dried in an oven for 1 hour at 100°C. From the loss in weight (i.e. 0.0100g) the product included 10% water content.

Characterization of the product crystals was accomplished by measuring the absorbance on the Shimadzu UV-Vis. From the UV-Vis spectra and % water content the product chemical formula was determined to be $\text{Ru}(\text{bipy})_3(\text{BF}_4)_2 \cdot 4\text{H}_2\text{O}$. Through the use of Beer-Lambert's equation 2 the purity was calculated with equation 3 to be 98% pure as shown below with the spectra shown in Figure 4. The MLCT absorption (Abs.= 0.91) at the λ_{max} of 453nm and $\epsilon_{\text{max}} = 14241 \text{ l mol}^{-1} \text{ cm}^{-1}$ was in agreement with literature values of 453nm^(5, 15), $\epsilon_{\text{max}} \approx 14600 \text{ l mol}^{-1} \text{ cm}^{-1}$ ⁽⁴⁾, for the $\text{Ru}(\text{bipy})_3(\text{BF}_4)_2$.

Beer-Lambert law: $A = \epsilon \ell c \rightarrow \epsilon = A / \ell c \rightarrow \epsilon = 0.91 / (1)(6.39 \times 10^{-5} \text{M}) = 14241 \text{ l mol}^{-1} \text{ cm}^{-1}$ [2]

A = absorbance

ϵ = molar absorptivity

ℓ = path length

c = concentration of absorbing species

% Purity = $\epsilon / \epsilon^\circ \times 100 \rightarrow 14241 / 14600 \times 100 = 98\% \text{ Pure}$ [3]

ϵ = experimental molar absorptivity

ϵ° = literature $[\text{Ru}(\text{bipy})_3]^{2+}$ molar absorptivity⁽⁴⁾

Preparation and Characterization of Dibromo-functionalized dimeric copper complex,

Cu_2L (Structure II)

The dibromo-functionalized dimeric copper (II) dichloride complex (Cu_2L^{2+}), $\text{C}_{22}\text{H}_{20}\text{Br}_2\text{Cu}_2\text{N}_4\text{O}_2^{2+}$, (2.23 mmol) shown as structure II was obtained from a previous study⁽¹⁶⁾.

The initial solution of 0.00223 M Cu_2L^{2+} was prepared by dissolving the complex (MW = 766 g/mol) in water. Into a 100 cm^3 volumetric flask, Cu_2L^{2+} , 0.1708 g (0.00223 mol) was brought up with DI to 100 cm^3 and dissolved. A range of Cu_2L^{2+} solutions were made up using the same procedure: 0.0214 g (0.279 mM), 0.0427 g (0.558 mM), 0.0640 g (0.836 mM), 0.0854 g (1.115 mM), 0.1025 g (1.338 mM), 0.1196g (1.561 mM), 0.1367g (1.784 mM), 0.1537 g (2.007 mM), & 0.1708 g (2.23 mM).

Characterization of a 0.00223M Cu_2L^{2+} complex was accomplished by measuring the absorbance on the Shimadzu 1700 UV-Vis spectrophotometer. The concentration was made up to give a $\epsilon = 89$ (d-d transition) at 607 nm. The λ_{max} and ϵ_{max} were in agreement with the previous study values of $\lambda_{\text{max}} = 606$ nm & $\epsilon_{\text{max}} = 93$ for the dibromofunctionalized copper complex, Cu_2L^{2+} .⁽¹⁶⁾

Preparation of 0.00446 M & 0.00223 M $[\text{Ru}(\text{bipy})_3]^{2+}$

Initial experiments involved 0.00446 M $[\text{Ru}(\text{bipy})_3](\text{BF}_4)_2 \cdot 4\text{H}_2\text{O}$ (MW = 569.37 g/mol). To conserve material the concentration of $[\text{Ru}(\text{bipy})_3]^{2+}$ was subsequently reduced to 0.00223 M. The 0.00446 M $[\text{Ru}(\text{bipy})_3]^{2+}$ solution was made up as follows. Into a 50 cm^3 volumetric flask, $[\text{Ru}(\text{bipy})_3](\text{BF}_4)_2 \cdot 4\text{H}_2\text{O}$, 0.1270 g (0.00446 mol) was brought up to 50 cm^3 with DI and dissolved. The 0.00223 M $[\text{Ru}(\text{bipy})_3]^{2+}$ solution was made up as follows. Into a 50 cm^3 volumetric flask, $[\text{Ru}(\text{bipy})_3](\text{BF}_4)_2 \cdot 4\text{H}_2\text{O}$, 0.0635 g (0.00223 mol) was brought up to 50 cm^3 with DI and dissolved. These solutions were

remade at 50 cm³ volume in the same manner but at constant ionic strength (0.1 M KNO₃) for quantitative studies.

Absorbance Measurements

UV-Vis absorption spectra of the following [Ru(bipy)₃]²⁺ - Cu₂L²⁺ mixtures were determined on the Shimadzu 1700 UV-Vis spectrophotometer: 1:1, 2:1, 3:1, 1:2, & 1:3 mole ratios. The mixtures were made by mixing the following cm³ of each [Ru(bipy)₃]²⁺ & Cu₂L²⁺ complexes together: 2 cm³ [Ru(bipy)₃]²⁺ to 2 cm³ Cu₂L²⁺, 4 cm³ [Ru(bipy)₃]²⁺ to 2 cm³ Cu₂L²⁺, 6 cm³ [Ru(bipy)₃]²⁺ to 2 cm³ Cu₂L²⁺, 2 cm³ [Ru(bipy)₃]²⁺ to 4 cm³ Cu₂L²⁺ & 2 cm³ [Ru(bipy)₃]²⁺ to 6 cm³ Cu₂L²⁺.

The absorption spectrum of a 1:1 mixture of [Ru(bipy)₃]²⁺ - Cu₂L²⁺ was also obtained after treating the mixture with a Blak-ray, UVL-56, long-wave UV-366nm lamp for 1 hour. A 1:1 [Ru(bipy)₃]²⁺ - Cu₂L²⁺ mixture was also looked at in 0.1M NaOH and in 0.1M H₂SO₄. Individually the [Ru(bipy)₃]²⁺ and Cu₂L²⁺ spectra were obtained in 0.1M H₂SO₄. A 1:1 mixture was also analyzed with an addition of 5 cm³ of 0.1M HCl. An absorption spectrum of the Cu₂L²⁺ complex with an addition of 5 cm³ of 0.1M HCl was taken as well.

A 2:1 Cu₂L²⁺ to [Ru(bipy)₃]²⁺ mixture in 0.1M KSCN was attempted but a solid precipitate formed. The precipitate was dissolved in 10 mL of HNO₃ then analyzed. The last absorbance spectra conducted with the Shimadzu 1700 UV-Vis spectrophotometer involved a sample consisting of 2 cm³ [Ru(bipy)₃]²⁺ + 2 cm³ Cu₂L²⁺ plus 2 mL of 3% H₂O₂.

Emission Analyses

Emission analyses were carried out on the Ocean Optics USB4000 UV-Vis spectrometer with a LS-450 blue LED pulsed light source. Temperature effects on the complexes were first examined. A 2:1 molar ratio of $[\text{Ru}(\text{bipy})_3]^{2+} - \text{Cu}_2\text{L}^{2+}$ was heated to 70°C , then the emission was studied while cooling. The experiment involved heating a 10 cm^3 2:1 molar sample on a hotplate while monitoring it with a thermometer. After reaching a temperature of 70°C , a 5 cm^3 sample was transferred to a cuvette and analyzed on the Ocean Optics spectrometer. In the first experiment the emission was recorded every 30 seconds for 12 minutes. For the following tests the thermometer was placed into a 10 cm^3 graduated cylinder containing the remaining 70°C heated sample that was not placed into the cuvette to record the temperature as it cooled at each emission recording. Emission from the Ocean Optics spectrometer and temperature readings from the thermometer in the graduated cylinder of the cooling sample were taken every 30 seconds until the thermometer cooled to a room temperature of 25°C . A series of temperature studies with the same above parameters were conducted using solutions with the following molar ratios of $[\text{Ru}(\text{bipy})_3]^{2+} - \text{Cu}_2\text{L}^{2+}$: 2:1, 2: 1.2, 2:1.4, 2:1.6, 2:1.8, & 2:2. The emission spectrum of a 2:1 molar sample at room temperature (i.e. no heating) was also obtained.

Emission spectra of solutions with the molar ratios listed in the previous paragraph were recorded at room temperature (i.e. 19°C) on the Ocean Optics

spectrometer with emission at 617 nm recorded under the same parameter settings. To investigate emission below the 2:1 molar ratio, three new $[\text{Ru}(\text{bipy})_3]^{2+}$ - Cu_2L^{2+} molar ratios were prepared: 2:0.25, 2:0.50, & 2:0.75. Using the same parameters on the Ocean Optics spectrometer the emission intensities for the three new ratios were recorded at the 617 nm at room temperature (i.e. 19°C). These three new molar ratios were run along with the $[\text{Ru}(\text{bipy})_3]^{2+}$ - Cu_2L^{2+} molar ratios of 2:1 to 2:2 on the Ocean Optics spectrometer.

To determine the effect of oxygen quenching on the $[\text{Ru}(\text{bipy})_3]^{2+}$ emission the 2:0.25, 2:0.50, & 2:0.75 $[\text{Ru}(\text{bipy})_3]^{2+}$: Cu_2L^{2+} molar ratio mixtures emission intensity was taken after purging samples with argon for 5 minutes and without purging the sample. The Ocean Optics spectrometer was set at the previous mentioned parameters. The emissions at 617 nm were recorded.

To maintain a constant ionic strength in the samples KCl and KNO_3 were investigated to determine if they had a effect on the $[\text{Ru}(\text{bipy})_3]^{2+}$ emission. Potassium chloride in the following amounts, 0.0030, 0.0046, & 0.0060g, was added to three different samples of the 0.00446M $[\text{Ru}(\text{bipy})_3]^{2+}$ to give 0.045, 0.069, & 0.089 M KCl. The emission spectra of these $[\text{Ru}(\text{bipy})_3]^{2+}$ based KCl samples were recorded on the Ocean Optics at 617 nm using the same previous parameters. These samples were compared to a 0.00446M $[\text{Ru}(\text{bipy})_3]^{2+}$ sample with no added electrolytes. Potassium chloride, KCl, was shown to reduce emission intensity. The experiment was repeated

with adding 0.0113g KNO₃ to a 0.00446M [Ru(bipy)₃]²⁺ only sample to give a 0.228 M KNO₃. Potassium nitrate, KNO₃, did not result in any reduced emission.

A [Ru(bipy)₃]²⁺ solution (2.223mM) was made up with KNO₃ (0.5056g, 0.1 M) and characterized on the Shimadzu 1700 UV-Vis spectrophotometer. Using the previously made Cu₂L²⁺ solutions, new 50 mL solutions with KNO₃ (0.5056g, 0.1 M) were made. As summarized in Table 1 the Cu₂L²⁺ solutions were in the following concentrations (mM): 0.279, 0.558, 0.836, 1.115, 1.338, 1.561, 1.784, 2.007, & 2.223.

Table 1. Cu₂L²⁺: [Ru(bipy)₃]²⁺ ratios in 0.1M KNO₃.

Cu ₂ L ²⁺ : [Ru(bipy) ₃] ²⁺ Ratio	Cu ₂ L ²⁺ (mM)	[Ru(bipy) ₃] ²⁺ (mM)
0.000	0.000	2.230
0.125	0.279	2.230
0.250	0.558	2.230
0.375	0.836	2.230
0.500	1.115	2.230
0.600	1.338	2.230
0.700	1.561	2.230
0.800	1.784	2.230
0.900	2.007	2.230
1.000	2.230	2.230

In an attempt to determine the activation parameters for the two regions, a series of Cu₂L²⁺: [Ru(bipy)₃]²⁺ molar ratios samples shown in Table 2 were run at different temperatures, 25°C, 30°C, & 40°C, on the Horiba Jobin Yvon UV-Vis spectrometer.

Table 2. $\text{Cu}_2\text{L}^{2+}:\text{[Ru(bipy)}_3\text{]}^{2+}$ ratios in 0.1M KNO_3 .

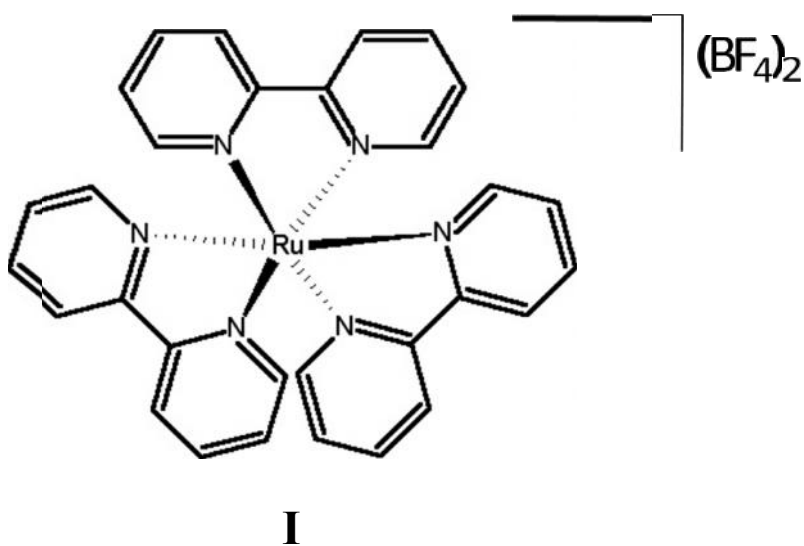
$\text{Cu}_2\text{L}^{2+}:\text{[Ru(bipy)}_3\text{]}^{2+}$ Ratio	Cu_2L^{2+} (mM)	$\text{[Ru(bipy)}_3\text{]}^{2+}$ (mM)
0.000	0	2.230
0.200	0.446	2.230
0.300	0.669	2.230
0.350	0.781	2.230
0.400	0.892	2.230
0.450	1.004	2.230
0.500	1.115	2.230
0.550	1.227	2.230
0.650	1.450	2.230
0.700	1.561	2.230
1.000	2.230	2.230

CHAPTER 3

RESULTS

The electronic absorption spectra were measured on the Shimadzu 1700 UV-Vis spectrophotometer. The experiments involved characterization of the synthesized $[\text{Ru}(\text{bipy})_3](\text{BF}_4)_2$ and the Cu_2L^{2+} complex as well as initial absorbance analyses of different mixture ratios of both. The $[\text{Ru}(\text{bipy})_3]^{2+}$ showed a λ_{max} at 453nm and ϵ_{max} of 14,241 $\text{l mol}^{-1} \text{cm}^{-1}$ while the Cu_2L^{2+} had a λ_{max} at 607nm and ϵ_{max} of 89 $\text{l mol}^{-1} \text{cm}^{-1}$. A weight loss experiment performed on the synthesized $[\text{Ru}(\text{bipy})_3]^{2+}$ showed it to have a water content of 4 H_2O to define the chemical formula to be $[\text{Ru}(\text{bipy})_3]^{2+}(\text{BF}_4)_2 \cdot 4\text{H}_2\text{O}$.

The synthesized $[\text{Ru}(\text{bipy})_3]^{2+}(\text{BF}_4)_2$ is shown as Structure I with its corresponding absorption spectra below it in Figure 4.



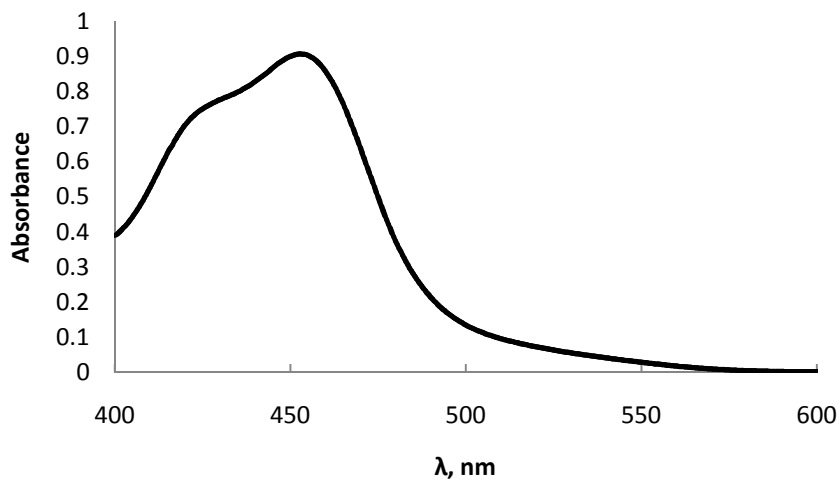
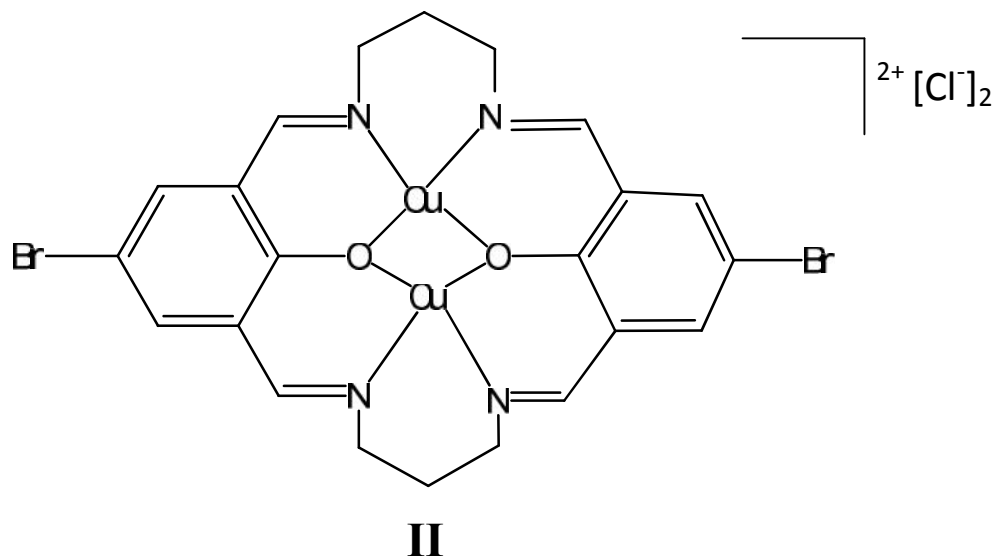


Figure 4. Absorption spectrum of $[\text{Ru}(\text{bipy})_3](\text{BF}_4)_2 \cdot 4\text{H}_2\text{O}$, $c = 8.92 \times 10^{-5} \text{ M}$, 25°C .

The Cu_2L^{2+} is shown below as Structure II with its corresponding absorption spectra below it in Figure 5. The complete molecular formula of Cu_2L^{2+} is $[\text{C}_{22}\text{H}_{20}\text{Br}_2\text{Cu}_2\text{N}_4\text{O}_2](\text{Cl}_2)$.



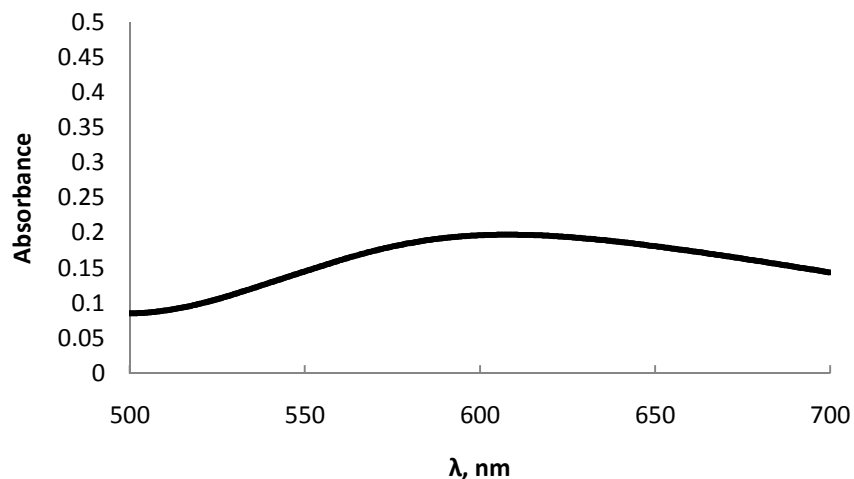


Figure 5. Absorption spectrum of Cu₂L, c = 2.23 mM, 25°C.

The electronic absorption spectral results of the experiments involving [Ru(bipy)₃]²⁺ and Cu₂L²⁺ plus the mixtures and different media analyzed with the Shimadzu 1700 UV-Vis spectrophotometer are appended in Table 3. The λ_{max} for the [Ru(bipy)₃]²⁺ and Cu₂L²⁺ do not shift upon mixing, indicating no reaction between the two complexes. In another attempt to react the compounds using different pH conditions, the mixtures were made up in 0.1M NaOH as well as a 0.1 M H₂SO₄ and 0.1 M HCl. These experiments also failed to produce reaction of the [Ru(bipy)₃]²⁺ with the Cu₂L²⁺, thus showing that it could not be pH induced at the levels attempted. Irradiating the [Ru(bipy)₃]²⁺ and Cu₂L²⁺ mixtures with a Blak-ray, UVL-56, long-wave UV-366nm light source prior to UV-Vis absorbance analyses again failed in inducing a reaction between the [Ru(bipy)₃]²⁺ and Cu₂L²⁺, which is indicated by the λ_{max} not shifting.

Because $[\text{Ru}(\text{bipy})_3]^{2+}$ is known to fluoresce, we decided to study the effect of Cu_2L^{2+} on the fluorescence of $[\text{Ru}(\text{bipy})_3]^{2+}$. Irradiation of $[\text{Ru}(\text{bipy})_3]^{2+}$ produces a charge-transfer excited species $^*[\text{Ru}(\text{bipy})_3]^{2+}$ that emits light at a higher wavelength than its absorption wavelength when excited by a UV light source.⁽¹⁵⁾ The $[\text{Ru}(\text{bipy})_3]^{2+}$ emission intensity ($\lambda = 617 \text{ nm}$) decreases linearly with increasing concentration of Cu_2L^{2+} and is also directly related to $[\text{Ru}(\text{bipy})_3]^{2+}$ that is present, see Figure 6. These experiments are based on a part to part ratio; therefore, when Cu_2L^{2+} increases, the $[\text{Ru}(\text{bipy})_3]^{2+}$ decreases in concentration. Lower $[\text{Ru}(\text{bipy})_3]^{2+}$ results in less emission but the influence of the Cu_2L^{2+} quenching effects was unknown. This unknown effect led into the investigation of the quenching effect of the dimeric copper complex on the $[\text{Ru}(\text{bipy})_3]^{2+}$. The Cu_2L^{2+} complex was not observed to fluoresce.

Quantitative studies investigating temperature effects on $[\text{Ru}(\text{bipy})_3]^{2+}$ emission were conducted on $[\text{Ru}(\text{bipy})_3]^{2+}$ and the Cu_2L^{2+} complex as well as mixtures of both using the Ocean Optics spectrometer. The mixtures were heated prior to emission analysis showing that heating reduced the $[\text{Ru}(\text{bipy})_3]^{2+}$ emission intensity and that cooling would reversibly return the emission intensity back to initial room temperature analysis levels. Higher temperature suppression of the emission is a result of a thermally populated excited state that decays more rapidly at higher temperature than one at lower temperature.⁽⁴⁾

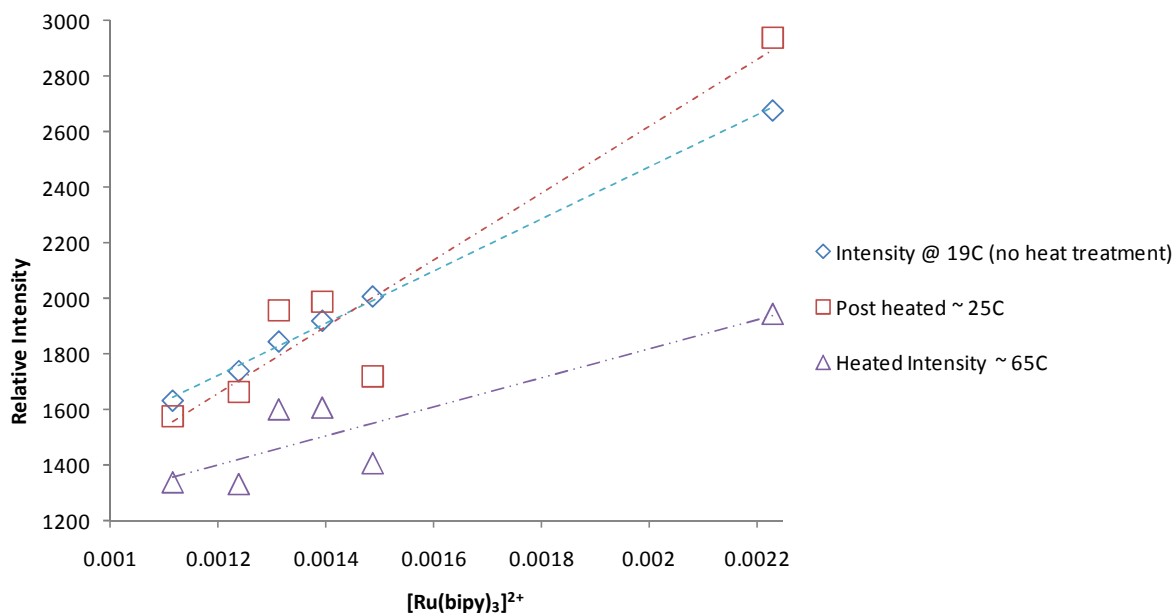


Figure 6. Emission intensity vs. $[\text{Ru}(\text{bipy})_3]^{2+}$ & temperature quantitative heating study results.

A literature search indicated that oxygen will quench $[\text{Ru}(\text{bipy})_3]^{2+}$ emission resulting in a lower emission intensity.⁽⁹⁾ Samples degassed with argon prior to analysis showed a higher emission intensity compared to the samples that were not degassed. This experiment validated that oxygen decreased the emission intensity as shown in Figure 7. All samples were therefore degassed with argon for 2 minutes prior to analysis to remove oxygen.

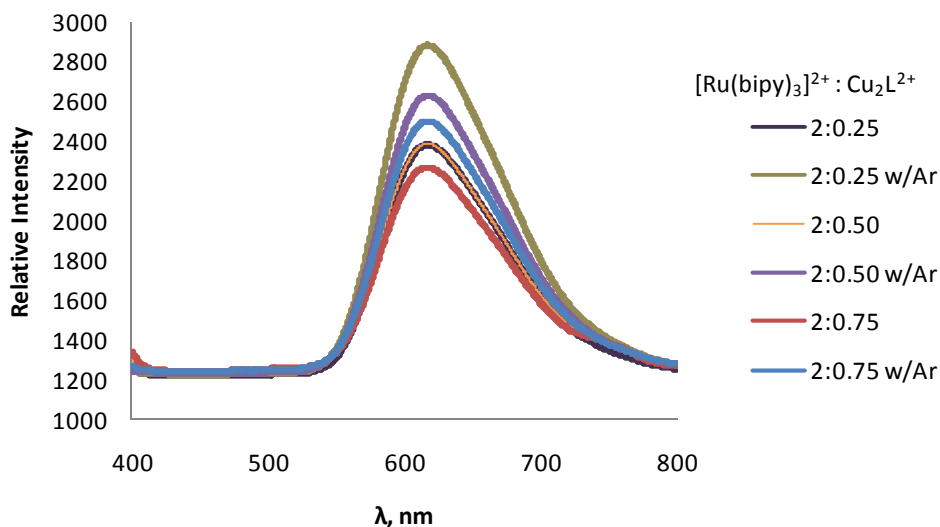


Figure 7. Comparison of Ar purged with non-purged $[\text{Ru}(\text{bipy})_3]^{2+} : \text{Cu}_2\text{L}^{2+}$ molar ratio samples.

To quantitatively study the effect of Cu_2L^{2+} on emission intensity, a fluorescence spectrum of a $[\text{Ru}(\text{bipy})_3]^{2+}$ solution with no Cu_2L^{2+} quencher present was obtained and was measured at $\lambda_{\text{max}} = 617\text{nm}$. Then solutions with increasing amounts of the Cu_2L^{2+} quencher were analyzed. The fluorescence intensities were seen to decrease as the concentrations of the quencher increased, shown in Table 4 and Figure 8. The samples were purged with argon for 2 minutes prior to emission intensity analyses on the Ocean Optics spectrometer using the same parameters as above maintaining constant pH and ionic strength.

Table 4. Measured fluorescence data for $\text{Cu}_2\text{L}^{2+}:\text{[Ru(bipy)}_3\text{]}^{2+}$ ratios in 0.1M KNO_3 , 25°C.

$\text{Cu}_2\text{L}^{2+}:\text{[Ru(bipy)}_3\text{]}^{2+}$ Ratio	Fluorescence Intensity
0.000	2680
0.125	2586
0.250	2365
0.375	2241
0.500	2011
0.600	1920
0.700	1845
0.800	1738
0.900	1693
1.000	1633

The fluorescence intensities are plotted against the corresponding mole ratios in Figure 8. As to be expected, the plot shows an emission decrease resulting from an increasing addition of the quencher Cu_2L^{2+} . The figure also indicates that a break occurs at the 0.5 $\text{Cu}_2\text{L}^{2+}:\text{[Ru(bipy)}_3\text{]}^{2+}$ molar ratio which is verified by higher R^2 for each of the individual segments ($R^2=0.983 < 0.5$ molar ratio & $R^2=0.986 > 0.5$ molar ratio) than the R^2 value if all the ratios are grouped together ($R^2=0.977$). To validate the results the experiment was repeated two times. Experimental results are shown in Table 5 with the first experiment results plotted in Figures 8 and 9. Results from repeated trials are appended in Tables 7 and 8.

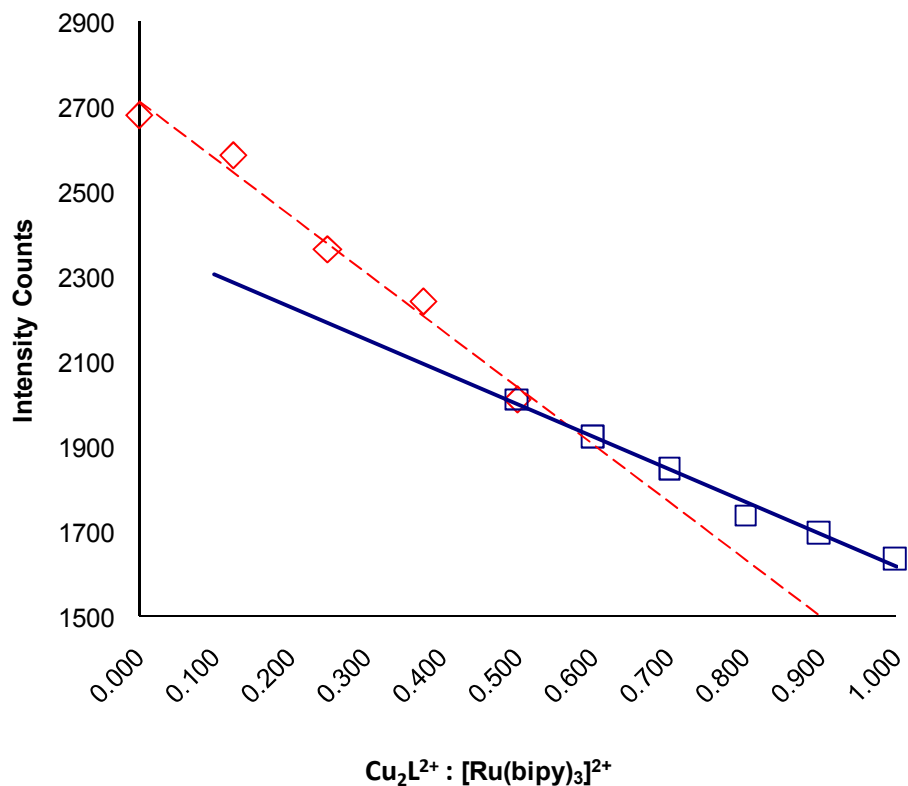


Figure 8. Emission intensity decrease as a result of Cu_2L^{2+} quenching on $[\text{Ru}(\text{bipy})_3]^{2+}$, 25°C. $[\text{Ru}(\text{bipy})_3]^{2+} = 2.23\text{mM}$.

From the $\text{Cu}_2\text{L}^{2+} : [\text{Ru}(\text{bipy})_3]^{2+}$ molar ratio vs. intensity plot (Figure 8) the I_0 for each segment of datapoints (i.e. < 0.5 molar ratio and > 0.5 molar ratio) was taken as the y-intercept for each of the segment's trendline. Using the y-intercept derived I_0 the relative fluorescence intensities using the Stern-Volmer, Equation 1, were plotted in 2 segments, 0 to 1.115mM Cu_2L^{2+} and 1.115 to 2.23mM Cu_2L^{2+} , corresponding to ratios < 0.5 and > 0.5 , respectively, as shown in Figure 9.

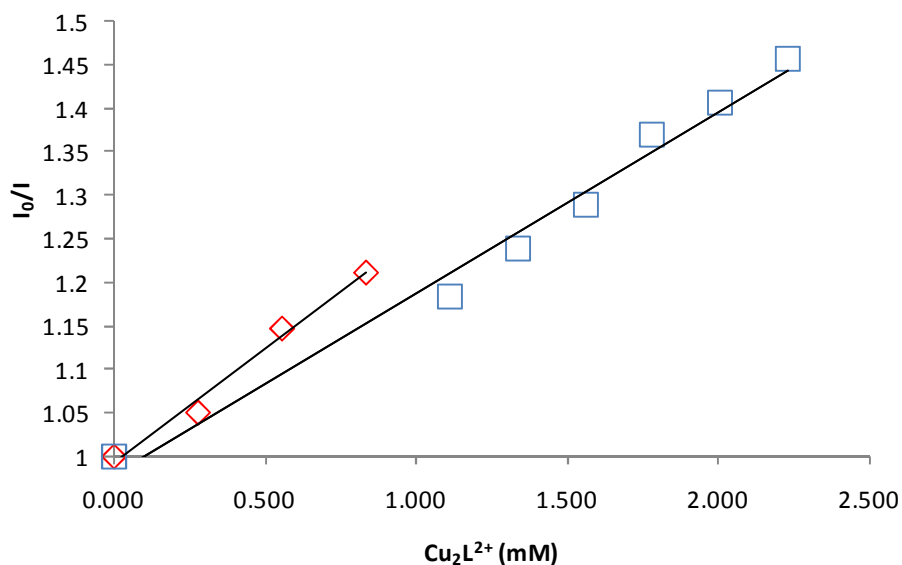


Figure 9. Stern-Volmer plot of the relative fluorescence intensities.

The slope of each line is the Stern-Volmer constant value of K_{sv} . Seddon et al.⁽⁴⁾ provide a series of τ (μs) for the fluorescence lifetime for $[\text{Ru}(\text{bipy})_3]^{2+}$ in water at 298K which have an average value of 0.633τ (μs). Using the K_{sv} and the fluorescence lifetime, the quenching rate constants (k_q) of Cu_2L^{2+} for the two segments were determined with the equation 4.

$$k_q = \frac{K_{sv} \nu}{\tau} \quad [4]$$

Table 5 shows the calculated rate constants for the quenching by Cu_2L^{2+} on $[\text{Ru}(\text{bipy})_3]^{2+}$ determined by equation 4.

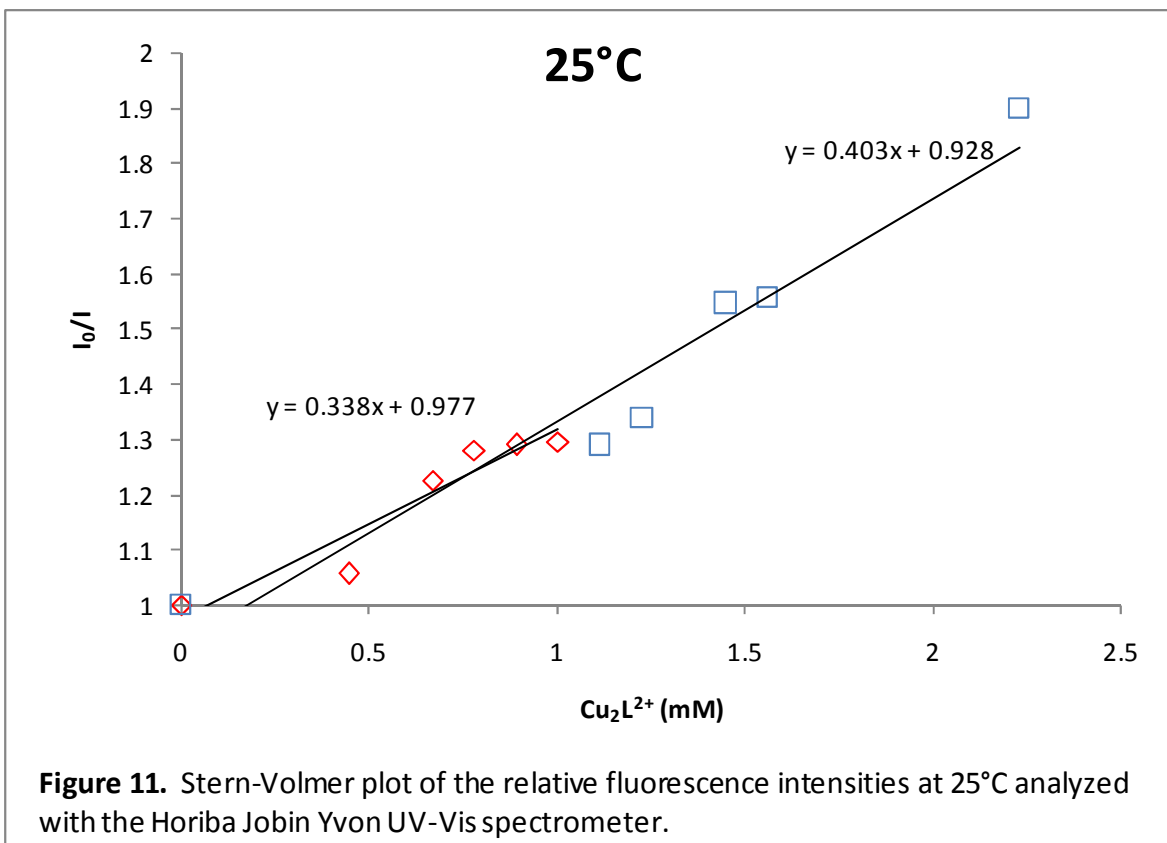
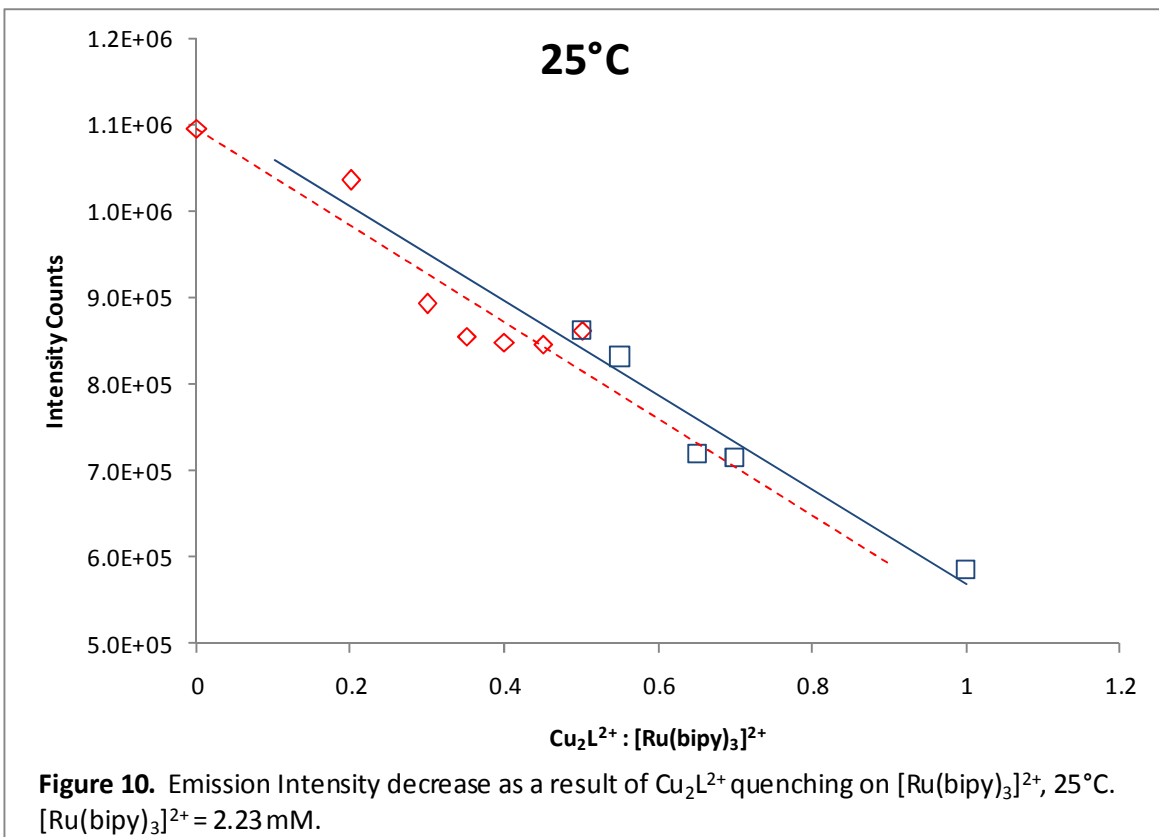
Table 5. Calculation of quenching rate constant (k_q) of Cu_2L^{2+} on $\text{Ru}(\text{bipy})_3^{2+}$ (2.23 mM), 25°C.

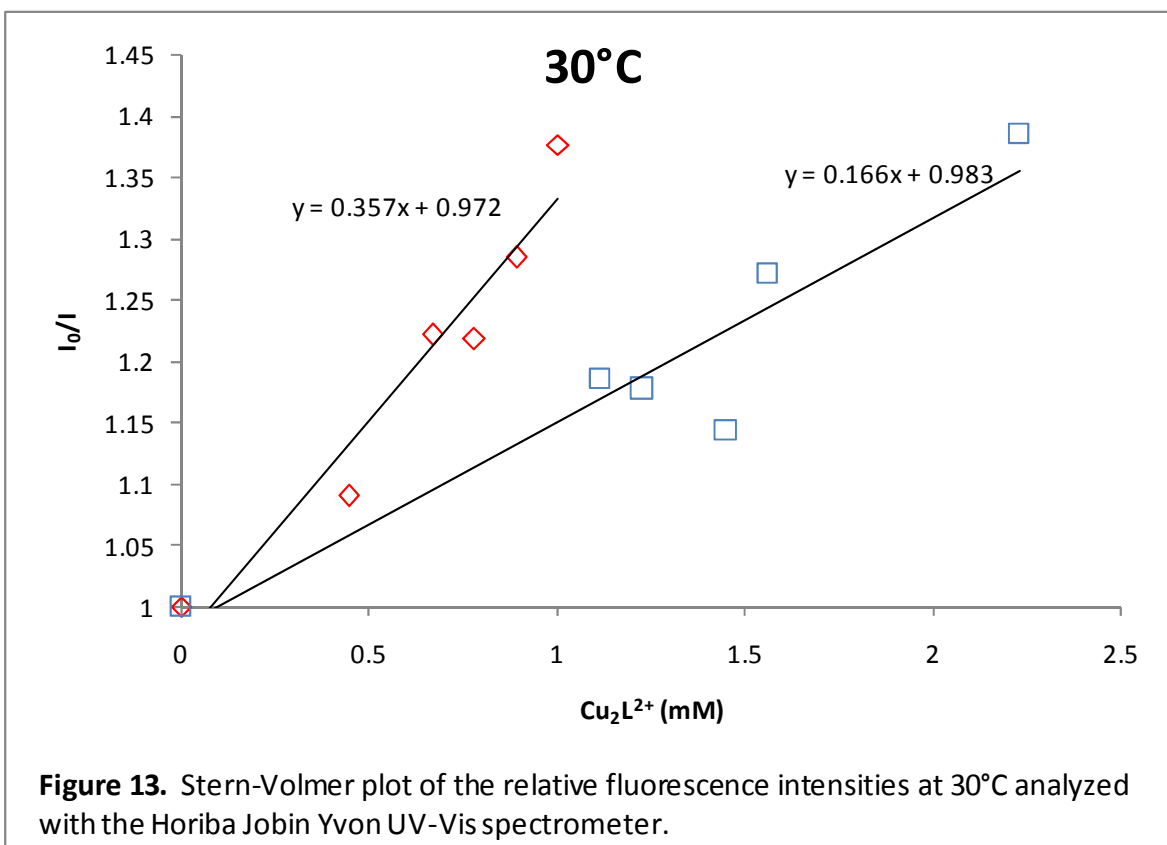
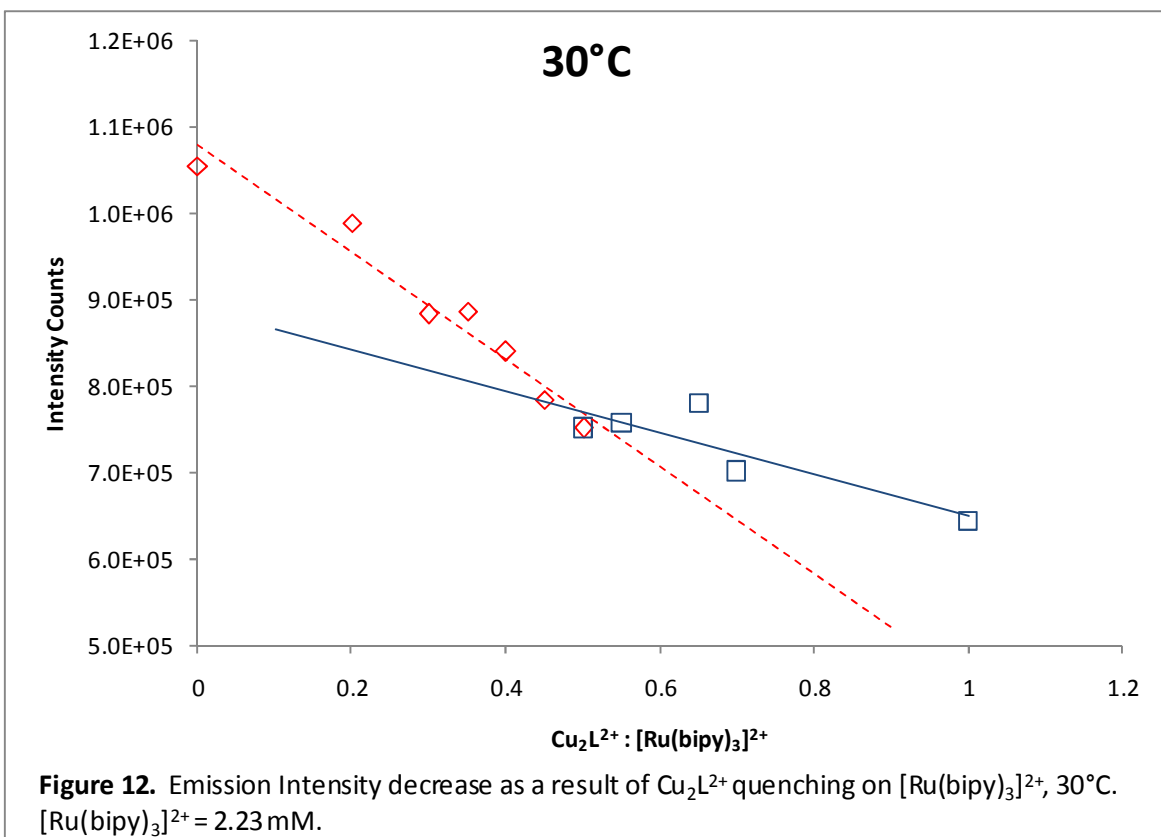
Experiment	Cu_2L^{2+} Conc. Range (mM)	K_{sv} (mM^{-1})	* k_q ($\times 10^6$) $\text{M}^{-1}\text{s}^{-1}$
1	0 - 0.836	0.261 ± 0.022	412
	1.115 - 2.23	0.208 ± 0.012	329
2	0 - 0.836	0.251 ± 0.034	397
	1.115 - 2.23	0.207 ± 0.012	327
3	0 - 0.836	0.222 ± 0.022	351
	1.115 - 2.23	0.212 ± 0.028	335
Average	0 - 0.836	0.245 ± 0.012	387
	1.115 - 2.23	0.209 ± 0.002	330

*Fluorescence lifetime for $\text{Ru}(\text{bipy})_3^{2+}$ calculated from average result (i.e. 0.633τ (μs) at 298K in H_2O).⁽⁴⁾

From Table 5 the calculated quenching rate constants (k_q) show that $<0.5 \text{Cu}_2\text{L}^{2+}$: $[\text{Ru}(\text{bipy})_3]^{2+}$ molar ratios the k_q of Cu_2L^{2+} on $[\text{Ru}(\text{bipy})_3]^{2+}$ is faster (avg = $387 \times 10^{-6} \text{M}^{-1}\text{s}^{-1}$) than the $\geq 0.5 \text{Cu}_2\text{L}^{2+}$: $[\text{Ru}(\text{bipy})_3]^{2+}$ molar ratios (avg = $330 \times 10^{-6} \text{M}^{-1}\text{s}^{-1}$). Schenk et al. reported a similar but slower quenching rate for $\text{Cu}(\text{aq})^{2+}$ on the fluorescence of $[\text{Ru}(\text{bipy})_3]^{2+}$ as $212 (\pm 83) \times 10^{-6} \text{M}^{-1}\text{s}^{-1}$.⁽³⁾

The spectra of the series of Cu_2L^{2+} : $[\text{Ru}(\text{bipy})_3]^{2+}$ molar ratios samples run at different temperatures, 25°C, 30°C, & 40°C, on the Horiba Jobin Yvon UV-Vis spectrometer are shown in Figures 10 to 15 with the data summarized in Table 6.





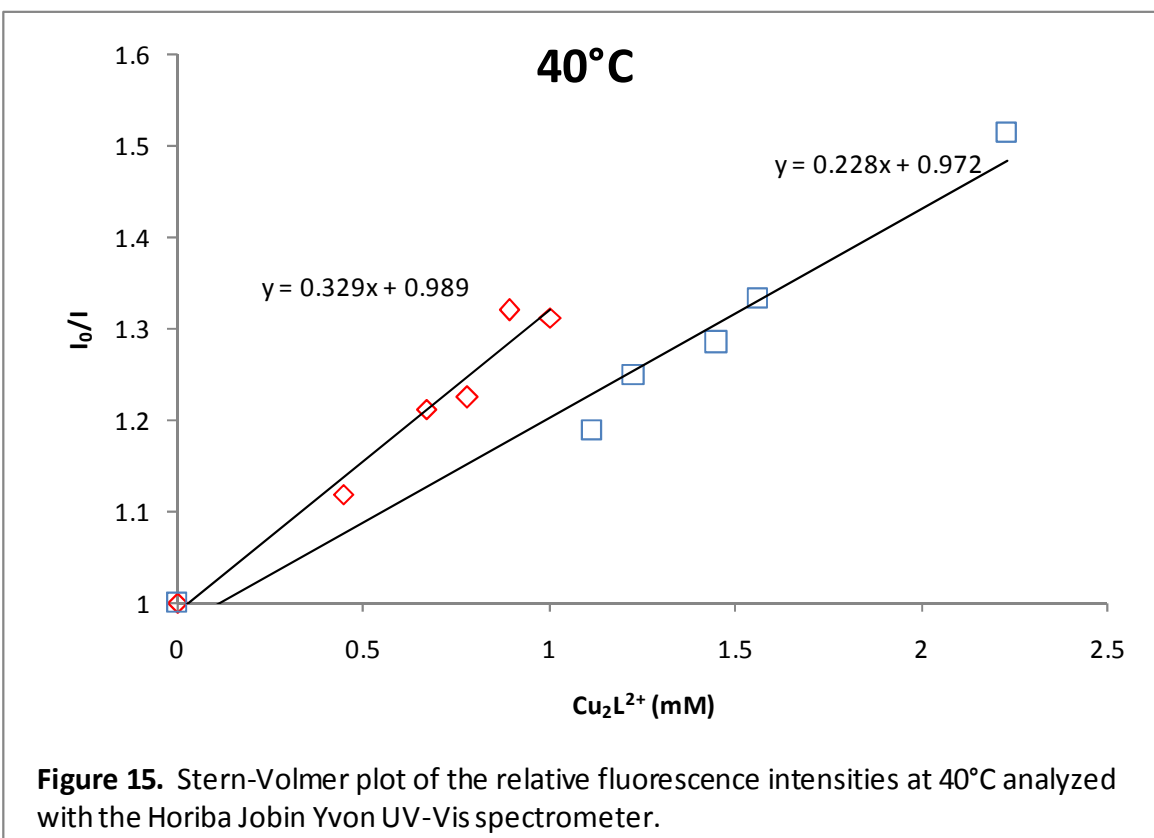
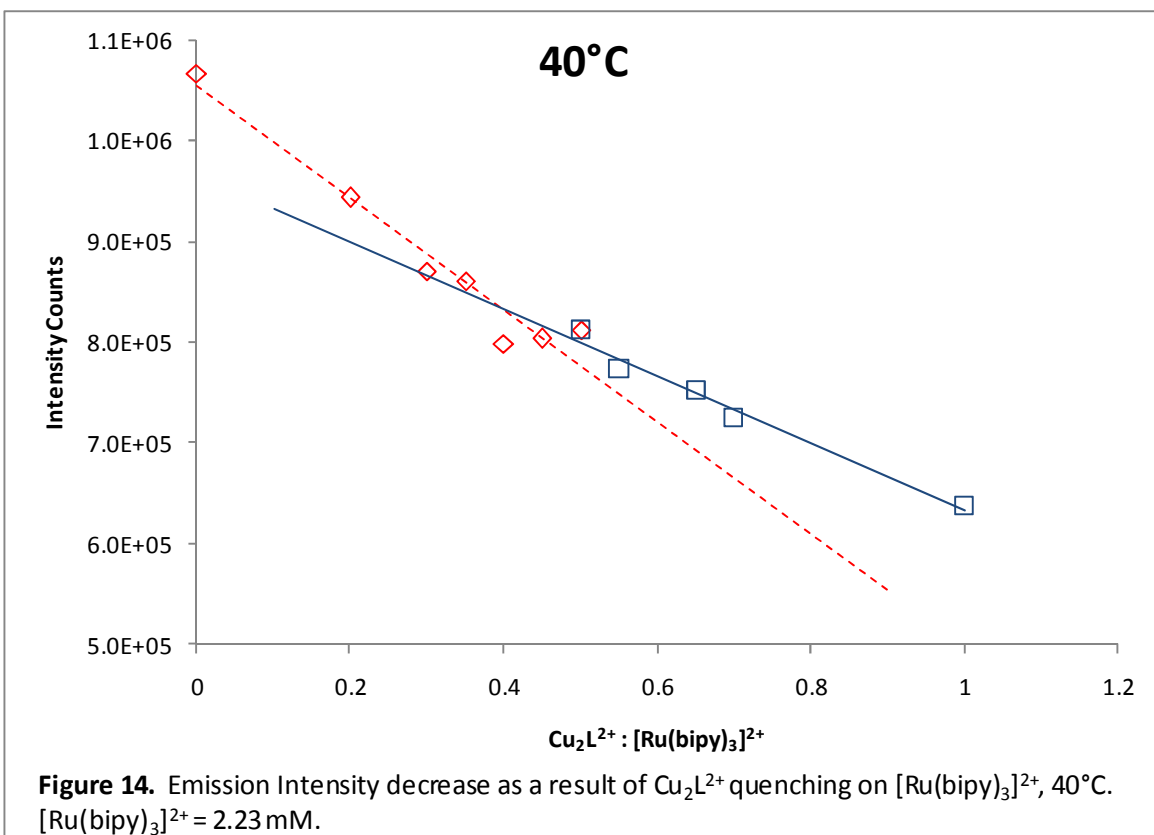


Table 6. Calculation of quenching rate constant (k_q) of Cu_2L^{2+} on $\text{Ru}(\text{bipy})_3^{2+}$. Horiba UV-Vis results.

Temperature (°C)	K_{sv} (mM^{-1}) (1)	$*k_q$ ($\times 10^6$) $\text{M}^{-1}\text{s}^{-1}$ (1)	K_{sv} (mM^{-1}) (2)	$*k_q$ ($\times 10^6$) $\text{M}^{-1}\text{s}^{-1}$ (2)
25	0.338	534	0.403	637
30	0.357	564	0.166	262
40	0.329	520	0.228	360

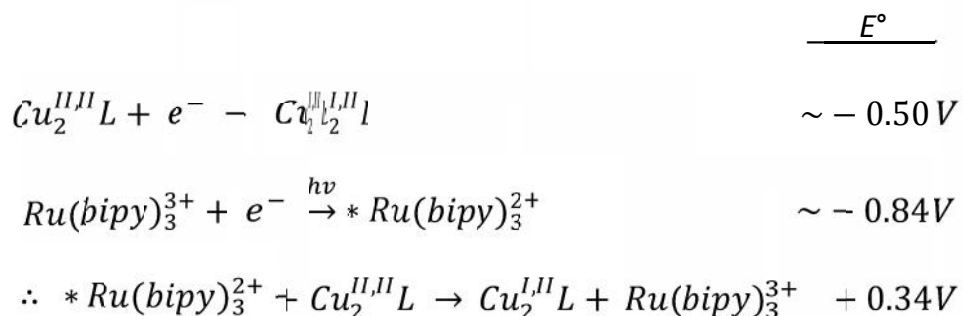
* Segment 1 for Cu_2 concentrations (mM) from 0 to 1.004, segment 2 for Cu_2 concentrations from 1.115 to 2.23. Fluorescence lifetime for $\text{Ru}(\text{bipy})_3^{2+}$ calculated from average result (i.e. 0.633 τ (μs) at 298K in H_2O .⁽⁴⁾

These experiments were conducted in an attempt to determine the activation parameters for the two regions. Duplicate runs at 30°C & 40°C confirmed the $k_q < 0.5$ $\text{Cu}_2\text{L}^{2+} : [\text{Ru}(\text{bipy})_3]^{2+}$ molar ratios of Cu_2L^{2+} on $[\text{Ru}(\text{bipy})_3]^{2+}$ being faster than the > 0.5 $\text{Cu}_2\text{L}^{2+} : [\text{Ru}(\text{bipy})_3]^{2+}$ molar ratios. As Figure 10 shows, the 25°C trial data points are too scattered to produce a confident trend; therefore, the trendlines could not indicate a break. It is unclear why the 25°C Horiba run failed to follow suit. No conclusive results could be obtained from these experiments performed on the Horiba Jobin Yvon UV-Vis spectrometer.

CHAPTER 4

DISCUSSION AND CONCLUSION

Initially the purpose of the experiment was to attempt to study possible electron transfer between the Cu_2L^{2+} to the $[\text{Ru}(\text{bipy})_3]^{2+}$ and provide for electron transport. However, no evidence of any oxidation-reduction between these two species was observed in their ground states. The $^*[\text{Ru}(\text{bipy})_3]^{2+}$ should react with the Cu_2L^{2+} via an oxidation-reduction pathway based on the following electrode potentials:



The E° for $\text{Cu}_2^{II,II}\text{L}$ is estimated from similar complexes.⁽¹⁷⁾

Using $\Delta G = -nF\Delta E$, the E° will be positive for a thermodynamically favored reaction. The reaction has to shift to the right to reach equilibrium so the oxidation of the $^*\text{Ru}(\text{bipy})_3^{2+}$ and reduction of the Cu_2^{II}L is favored. However, quenching from collision alone cannot be ruled out.

While electron transfer between the Cu_2L^{2+} to the $[\text{Ru}(\text{bipy})_3]^{2+}$ is still the ultimate goal, this experiment serves to characterize the quenching mechanics of the Cu_2L^{2+} on the $[\text{Ru}(\text{bipy})_3]^{2+}$. A review of the literature showed no studies of quenching by copper dimers on $[\text{Ru}(\text{bipy})_3]^{2+}$ emission.

Although the initial experiments failed to show any reaction between the Cu_2L^{2+} to the $[\text{Ru}(\text{bipy})_3]^{2+}$ many findings, and what we believe, through a review of literature, to be novel results were found. In addition to the break that is seen to occur at the 0.5 $\text{Cu}_2\text{L}^{2+} : [\text{Ru}(\text{bipy})_3]^{2+}$ molar ratio, we have shown that that the reaction of the Cu_2L^{2+} with the $[\text{Ru}(\text{bipy})_3]^{2+}$ is independent of pH at room temperature. Through determination that KCl can quench $[\text{Ru}(\text{bipy})_3]^{2+}$ and is therefore not suitable for addition to establish constant ionic strength, it suggests that halogens might quench $[\text{Ru}(\text{bipy})_3]^{2+}$. Another interesting finding is that heating reduced the $[\text{Ru}(\text{bipy})_3]^{2+}$ emission intensity and that cooling would reversibly return the emission intensity back to initial room temperature analysis levels. Through spectral comparison we also verified that oxygen quenches the fluorescence of $[\text{Ru}(\text{bipy})_3]^{2+}$.

The experiments performed show that Cu_2L^{2+} has a unique and novel quenching scheme with $[\text{Ru}(\text{bipy})_3]^{2+}$. Through the use of the Stern-Volmer relation we have shown that when Cu_2L^{2+} quenches the $[\text{Ru}(\text{bipy})_3]^{2+}$ a break occurs at the 0.5 $\text{Cu}_2\text{L}^{2+} : [\text{Ru}(\text{bipy})_3]^{2+}$ molar ratio and have also successively determined the rate constants of the quenching before and after the break. The Stern-Volmer equation models what is called dynamic quenching.⁽¹⁰⁾ Dynamic quenching is defined as quenching that occurs by the quencher, in this case, Cu_2L^{2+} , diffusing through solution and interacting with fluorescent species, in this case, $^*[\text{Ru}(\text{bipy})_3]^{2+}$, resulting in a deactivation of the excited state. The presence of quencher now adds another deactivation pathway in competition with

fluorescence in addition to any other deactivation pathways that were present before the introduction of the quencher. Therefore the emission intensity will be reduced. Dynamic quenching is controlled by how fast the quencher can diffuse through solution and “collide” with fluorescent species so in solutions it is very efficient.⁽¹⁸⁾ The quenching rate constants (k_q) of Cu_2L^{2+} on $[\text{Ru}(\text{bipy})_3]^{2+}$ were found to be $387 \times 10^{-6} \text{ M}^{-1}\text{s}^{-1}$ (avg. of 3 trials) below the 0.5 $\text{Cu}_2\text{L}^{2+} : [\text{Ru}(\text{bipy})_3]^{2+}$ ratio and $330 \times 10^{-6} \text{ M}^{-1}\text{s}^{-1}$ (avg. of 3 trials) above the 0.5 $\text{Cu}_2\text{L}^{2+} : [\text{Ru}(\text{bipy})_3]^{2+}$ ratio (Table 5).

The reason for the break is unclear, but we believe stoichiometry must play a decisive role in the quenching rate due to the following. With the quencher, Cu_2L^{2+} , being of a dimeric nature, we believe the break and decrease in quenching reaction rate above the 0.5 $\text{Cu}_2\text{L}^{2+} : [\text{Ru}(\text{bipy})_3]^{2+}$ molar ratio can be explained in terms of the stoichiometry. In terms of the stoichiometry, when the $\text{Cu}_2\text{L}^{2+} : [\text{Ru}(\text{bipy})_3]^{2+}$ ratio is <0.5 , then each $[\text{Ru}(\text{bipy})_3]^{2+}$ can interact with 1 Cu_2L^{2+} dimer. At 0.5 then there is exactly a 1:1 ratio $\text{Ru}^{\text{II}} : \text{Cu}^{\text{II}}$. Above the 0.5 ratio the $[\text{Ru}(\text{bipy})_3]^{2+}$ can interact with maybe only one of the Cu_2L^{2+} 's in the dimer, or with a $[\text{Ru}(\text{bipy})_3]^{2+} : \text{Cu}_2\text{L}^{2+}$ unit, so the quenching is less efficient.

Due to significant error in the variable temperature data taken on the Horiba Jobin Yvon UV-Vis spectrometer, these results are less conclusive, although the break is still evident.

CHAPTER 5

RECOMMENDATION

More investigation should be applied to determining the cause of the break at the 0.5 $\text{Cu}_2\text{L}^{2+} : [\text{Ru}(\text{bipy})_3]^{2+}$ molar ratio. These experiments could also involve looking into other dimeric quenchers and if they contain a break as well. A temperature study for the determination the activation parameters is still warranted due to our inconclusive results. An extension of the molar ratios would also be interesting to see if a trend exists for the break occurrence.

REFERENCES

1. Holler, F.; Skoog, D.; Crouch, S. *Principles of Instrumental Analysis*. Brooks/Cole, KY, **2006**.
2. Drago, R. *Physical Methods for Chemists*. Surfside, FL, **1992**, 113-117.
3. Schenk, J. and Sherer, D. *J. Phys. Chem. Lab* **2006**, *10*, 50-54.
4. Seddon, E. and Seddon, K. *The chemistry of ruthenium*. Elsevier, N.Y. **1984**, 1173-1260.
5. Jordan, R. *Reaction mechanisms of inorganic and organometallic systems*. Oxford University Press, N.Y. **1998**, 235-236.
6. Vos, J. and Kelly, J. *Dalton. Trans.*, 2006, 4869 – 4883. (The Photochemistry Portal, www.photochemistry.wordpress.com)
7. Sutin, N. and Creutz, C. *J. Chem. Ed.* **1983**, *60*, 809-814.
8. Francis, P.; Papettas, D.; Zammit, E.; Barnett, N. *Talanta* **2010**, *82*, 859-862.
9. Rusak, D.; James, W; Ferzola, M.; Stefanski, M. *J. of Chem. Ed.* **2006**, *83*, 1857-1859.
10. USB4000 Fiber Optic Spectrometer Installation and Operation manual, Document number 211-00000-000-02-0908, Ocean Optics, Inc. World Headquarters, Dunedin, FL, **2008**.
11. Cotton, F. *Advanced inorganic chemistry*. John Wiley & Sons, N.Y. **1980**, 922-924.

12. SpectraSuite Installation and Operation Manual

Document number 000-20000-300-02-201101, Ocean Optics, Inc. World Headquarters, Dunedin, FL, **2009**.

13. Valeur, B. and Berberan-Santos, M. *J. Chem. Educ.*, **2011**, *88* (6), 731–738.

14. Broomhead, J.; Young, C. *Inorg. Syn.* **1990**, *28*, 338-340.

15. Cola, L.; Prodi, L.; Zaccheroni, N.; Konig, B. *Inorganica Chimica Acta* **2002**, *336*, 1-7.

16. Moody, S. "Towards the design and synthesis of novel supramolecular triads comprising single Robson-type macrocyclic dicopper(II) cores flanked by two covalently linked terminal polypyridyl ruthenium(II) units." *MS thesis*, ETSU, **2008**.

17. Mandal, S. and Nag, K. *J. Chem. Soc. Dalton Trans.* **1983**, 2429-2434.

18. Valeur B. *Molecular Fluorescence: Principles and Applications*, Wiley, Weinheim, **2002**.

19. Pearson, P.; Bond, A.M.; Deacon, G.B.; Forsyth, C.; Spiccia, L. *Inorg. Chim. Acta* **2008**, *361*, 601-612.

20. Isoda, N.; Torii, Y.; Okada, T.; Misoo, M.; Yokoyama, H.; Ikeda, N.; Nojiri, M.; Suzuki, S.; Yamaguchi, K. *Dalton Trans.* **2009**, 10175-10177.

APPENDICES

Appendix A: UV-Vis Absorbance Tests Results

Table 3. UV-Vis absorbance test results

Sample ID	Description	UV-Vis Absorbance (nm)	
		[Ru(bipy) ₃] ²⁺ : 453 (~442)	Cu ₂ : 607
[Ru(bipy)₃]²⁺ (09-15-001) - Cu₂ (09-22-001) mixtures (part to part not molar ratios)			
09-22-003	1:1	0.42	0.09
09-22-004	2:1	0.46	0.06
09-22-005	3:1	0.48	0.05
09-22-006	1:2	0.37	0.13
09-22-007	1:3	0.35	0.14
[Ru(bipy)₃]²⁺ (09-15-001) - Cu₂ (09-22-001) mixtures with pre-analysis UV light exposure (part to part ratios)			
09-22-003-2	1:1	0.40	0.09
10-10-001	1:1	0.37	0.09
[Ru(bipy)₃]²⁺ (10-10-002, the 0.2 abs. [Ru(bipy)₃]²⁺ complex) - Cu₂ (09-22-001) mixtures in NaOH and H₂SO₄ media (part to part ratios)			
10-13-003	1:1 in 0.1M NaOH	0.22	0.14
10-13-004	1:1 in 0.1M H ₂ SO ₄	1.58	0.03
[Ru(bipy)₃]²⁺ (09-15-001) - Cu₂ (09-22-001) mixtures in NaOH and H₂SO₄ media with pre-analysis UV light exposure (part to part ratios)			
10-13-005	1:1	0.39	0.25
10-13-006	1:1	0.17	0.03
[Ru(bipy)₃]²⁺ (10-10-002, the 0.2 abs. [Ru(bipy)₃]²⁺ complex) - Cu₂ (09-22-001) mixtures in H₂SO₄ media (part to part ratios)			
10-21-001	1:1 [Ru(bipy) ₃] ²⁺ (4 cm ³) - Cu ₂ (4 cm ³) in H ₂ SO ₄	2.94	0.03
10-21-002	[Ru(bipy) ₃] ²⁺ (10-10-002) in H ₂ SO ₄	0.22	0.00
10-21-003	Cu ₂ (09-22-001) in H ₂ SO ₄	3.07	0.06
10-21-004	2nd run of 10-21-001 after 40 min.	0.20	0.03
[Ru(bipy)₃]²⁺ (10-10-002, the 0.2 abs. [Ru(bipy)₃]²⁺ complex) - Cu₂ (09-22-001) mixtures in HCl, KSCN (+ HNO₃), & H₂O₂ media (part to part ratios)			
10-21-005	1:1 + HCl	1.94	0.02
10-21-006	Cu ₂ + HCl	3.01	0.03
10-27-001	Cu ₂	---	0.19
10-27-002	Cu ₂ (4 cm ³) + KSCN + Ru (2 cm ³) + HNO ₃	*--- (1.03)	---
10-27-003	Cu ₂ (2 cm ³) + Ru (2 cm ³) + 3% H ₂ O ₂ (2 cm ³)	0.15	0.07
10-27-004	Rerun of 10-27-002	*0.26 (0.40)	0.15
[Ru(bipy)₃]²⁺ (11-07-002, 4.46x10⁻³M) - Cu₂ (09-22-001, 2.23x10⁻³M) mixtures (molar ratios)			
11-07-001	0.00223M Cu ₂ complex (09-22-001)	---	0.19
11-07-002	0.00446M [Ru(bipy) ₃] ²⁺	3.14	---
11-07-003	2:1	3.14	0.11
11-07-004	10x dilution of 11-07-003	2.12	0.01

*Potassium thiocyanate, KSCN, plus HNO₃ experiments which had λ_{max} of 442nm but this minor shift change was not considered an indication of the [Ru(bipy)₃]²⁺ - Cu₂L²⁺ complexing together.

Appendix B: Measured fluorescence data for $\text{Cu}_2\text{L}^{2+}:\text{[Ru(bipy)}_3\text{]}^{2+}$ ratios
in 0.1M KNO_3 , 25°C (1st Repeat)

Table 7. Measured fluorescence data for $\text{Cu}_2\text{L}^{2+}:\text{[Ru(bipy)}_3\text{]}^{2+}$ ratios in 0.1M KNO_3 , 25°C (1st Repeat)

$\text{Cu}_2\text{L}^{2+}:\text{[Ru(bipy)}_3\text{]}^{2+}$ Ratio	1st Repeat: Fluorescence Intensity
0.000	2488
0.125	2378
0.250	2191
0.375	2136
0.500	2085
0.600	1995
0.700	1927
0.800	1828
0.900	1763
1.000	1690

Appendix C: Measured fluorescence data for $\text{Cu}_2\text{L}^{2+}:\text{[Ru(bipy)}_3\text{]}^{2+}$ ratios
in 0.1M KNO_3 , 25°C (2nd Repeat)

Table 8. Measured fluorescence data for $\text{Cu}_2\text{L}^{2+}:\text{[Ru(bipy)}_3\text{]}^{2+}$ ratios in 0.1M KNO_3 , 25°C (2nd Repeat)

$\text{Cu}_2\text{L}^{2+}:\text{[Ru(bipy)}_3\text{]}^{2+}$ Ratio	2nd Repeat: Fluorescence Intensity
0.000	2380
0.125	2328
0.250	2157
0.375	2090
0.500	2063
0.600	1957
0.700	1800
0.800	1738
0.900	1813
1.000	1613

VITA

Kevin E. Cummins

- Personal Data: Date of Birth: March 26, 1970
 Place of Birth: Johnson City, Tennessee
 Marital Status: Married
- Education: Public Schools, Johnson City, Tennessee
 B.S. Double Major: Chemistry and History, East
 Tennessee State University, Johnson City,
 Tennessee 1995
 M.S. Chemistry, East Tennessee State University,
 Johnson City, Tennessee 2011
- Professional Experience: Lab Technician, Unimin Corporation, Spruce Pine,
 North Carolina, 1996-1997
 Senior Analytical Chemist, Unimin Corporation, Red
 Hill, North Carolina, 1997-2002
 Quality Assurance Specialist, King Pharmaceuticals,
 Bristol, Tennessee, 2002-2005
 Materials Analyst, Micron, Manassas, Virginia, 2005-
 2005
 Researcher, Unimin Corporation, Red Hill, North
 Carolina, 2006-present